HHS Public Access

Author manuscript

Brain Behav Immun. Author manuscript; available in PMC 2024 November 01.

Published in final edited form as:

Brain Behav Immun. 2023 November ; 114: 438–452. doi:10.1016/j.bbi.2023.09.009.

Sex differences in microglia function in aged rats underlie vulnerability to cognitive decline

Louise M. Ince[a], **Jeffrey S. Darling**[a], **Kevin Sanchez**[a], **Kiersten S. Bell**[a], **Jennifer K. Melbourne**[a], **Lourdes K. Davis**[a,b], **Kimberly Nixon**[a], **Andrew D. Gaudet**[b,c,d], **Laura.K. Fonken**[a,b,*]

[a]Division of Pharmacology & Toxicology, College of Pharmacy, University of Texas at Austin, Austin, TX 78712, USA

[b]Institute for Neuroscience, University of Texas at Austin, Austin, TX 78712, USA

[c]Department of Psychology, University of Texas at Austin, Austin, TX 78712, USA

[d]Department of Neurology, Dell Medical School, University of Texas at Austin, Austin, TX 78712, USA

Abstract

Aging is associated with a significant shift in immune system reactivity ("inflammaging"), as basal inflammation increases but protective responses to infection are compromised. The immune system exhibits considerable sex differences, which may influence the process of inflammaging, including immune cell activation and behavioral consequences of immune signaling (i.e., impaired memory). Here, we test the hypothesis that sex differences in immune aging may mediate sex differences in cognitive decline. Aged male and female rats received peripheral immune stimulation using lipopolysaccharide (LPS), then molecular, cellular, and behavioral outcomes were assessed. We observed that LPS-treated aged male rats showed cognitive impairment and increased neuroinflammatory responses relative to adult males. In contrast, aged female rats did not display these aging-related deficits. Using transcriptomic and flow cytometry analyses, we further observed significant age- and sex-dependent changes in immune cell populations in the brain parenchyma and meninges, indicating a broad shift in the neuroinflammatory environment that may potentiate these behavioral effects. Ovariectomized aged female rats were also resistant to inflammation-induced memory deficits, indicating that ovarian hormones are not required for the attenuated neuroinflammation in aged females. Overall, our results indicate that males have amplified inflammatory priming with age, which contributes to age-associated cognitive decline. Our findings highlight sexual dimorphism in mechanisms of aging, and suggest that sex is a crucial consideration for identifying therapies for aging and neuroinflammation.

*Corresponding author at: Division of Pharmacology & Toxicology, College of Pharmacy, University of Texas at Austin, Austin, TX 78712, USA. laura.fonken@austin.utexas.edu (Laura.K. Fonken).

Declaration of Competing Interest

The authors declare that they have no known competing financial interests or personal relationships that could have appeared to influence the work reported in this paper.

Appendix A. Supplementary data

Supplementary data to this article can be found online at https://doi.org/10.1016/j.bbi.2023.09.009.

Keywords

Neuroinflammation; Aging; Sex differences; Microglia; Behavior

1. Introduction

Inflammatory setpoints change with advancing age: basal inflammation is increased in the elderly, whereas response to infections or vaccinations are generally weakened as the body exhibits age-related immunosenescence, also known as “inflammaging” (Lord, 2013; Sasaki et al., 2011). Changes in peripheral immune function are also replicated in the central nervous system, resulting in age-associated neuroinflammation which can modulate neural function and behavior (Scheiblich et al., 2020). While the process of immunosenescence occurs in both sexes, previous research indicates that sex differences in immune aging may contribute to the differences observed in longevity and cognitive aging between men and women (Hirokawa et al., 2013).

Significant sexual dimorphism is present in multiple features of immune function and occurs across the lifespan (Klein and Flanagan, 2016). In general, women are more likely than men to be diagnosed with autoimmune diseases, such as multiple sclerosis or rheumatoid arthritis (Gleicher and Barad, 2007), and respond more strongly to vaccination (Fischinger et al., 2019). Women are also more likely to be diagnosed with age-associated neurodegenerative diseases such as Alzheimer’s disease (2022 Alzheimer’s disease facts and figures, 2022), although this is partially explained by the longer lifespan. The underlying relationship between immune activation and cognitive decline is complex, however, as women show higher cognitive reserve but faster cognitive decline than men (Levine et al., 2021). In parallel, rodent models of neuroinflammation have revealed sexual dimorphism in immunoregulatory mechanisms that underpin disease progression, such as increased immune cell infiltration and exacerbated demyelination in females in experimental autoimmune encephalomyelitis (Wiedrick et al., 2021), and increased influx of myeloid cells and proliferation of microglia in males following traumatic brain injury (Doran et al., 2019). These sex differences in pathophysiology may be mediated by divergent inflammatory mechanisms, yet the cellular and molecular substrates eliciting sex differences with age remain unresolved.

Sensitization or “priming” of the neuroimmune system occurs in male rodents with age and contributes to cognitive dysfunction: hippocampal microglia from aged male rodents exhibit more robust and prolonged cytokine responses following an immune challenge (Fonken et al., 2016b; Frank et al., 2010) and this is reflected in a specific impairment of hippocampal-dependent memory consolidation (Barrientos et al., 2006). Importantly, inhibiting inflammatory pathways that cause microglia priming in aged male rats can prevent cognitive impairments (Fonken et al., 2016b). Importantly, microglia priming in response to physiological stressors is not consistent between male and female rodents (Fonken et al., 2018b). Thus, here, we sought to understand whether female rats exhibited a similar age-associated exacerbation of neuroinflammation compared to male rats. Using intraperitoneal administration of lipopolysaccharide (LPS), we explored the links between

peripheral immune activation, neuroinflammatory responses, and age-associated cognitive changes in male and female rats. We report that whilst aged male rats showed cognitive impairment and increased neuroinflammatory responses relative to adult males, this was not evident in aged female rats. Our results indicate a sex-specific effect of microglia priming and neuroinflammatory potentiation with age, which contributes to age-associated cognitive decline in males but not in females.

2. Methods

2.1. Animal husbandry

All experiments were performed in adult (3 months) and aged (24 months) male and female Fisher 344 × Brown Norway (F344 × BN) F1 rats from the National Institute on Aging colony housed at Charles River. Room conditions were maintained at 22±2 °C with a 12:12 light:dark cycle with lights on at 0700 h. Animals were pair-housed in solid-bottom polycarbonate cages on corn cob bedding with access to food (Purina rodent chow [5LL2] Prolab RMH 1800) and reverse osmosis filtered water *ad libitum*. Rats were acclimated for at least seven days prior to any experimental manipulation. All experimental protocols were approved by The University of Texas at Austin Institutional Animal Care and Use Committee and performed in accordance with ARRIVE guidelines.

2.2. In vivo inflammatory challenge

To test inflammatory responses *in vivo*, rats were injected intraperitoneally (i.p.) with lipopolysaccharide (LPS; E. coli serotype 0111:B4; Sigma) or sterile saline as a vehicle control. Rats received 30 μg, 40 μg, and 60 μg injections of LPS for the initial fear conditioning experiments and the 40 μg dose of LPS was used in all subsequent experiments. Dose was not adjusted for body mass as administration of the same dose to all animals is the more conservative measure due to the increased body mass in aged animals (Supplemental Fig. S1A) – if LPS dose was adjusted to body mass, aged males would receive a substantially higher exposure (Barrientos et al., 2006). All animals were monitored for weight loss and lethargy following injections, indicative of a sickness response.

2.3. Fear conditioning

Rats underwent a contextual fear conditioning paradigm 48 h following i.p. LPS or saline injection (Barrientos et al., 2006; Fonken et al., 2016b; Fonken et al., 2018a). Rats were placed in a fear conditioning chamber (Ugo Basile) and baseline freezing behavior was scored by 2 condition-blind observers. After 2 min, rats received a 2 sec, 1.5 mA shock and then were returned to their home cage. 48 h later, rats were tested for freezing behavior over a period of 6 min as an indication of memory in the conditioned chamber. Rats were also subsequently tested in a control chamber (with modified floor and walls to distinguish from the test chamber).

2.4. Hippocampal gene expression analysis

Rats received a lethal overdose of Euthasol® Euthanasia Solution (pentobarbital sodium and phenytoin sodium) and then were transcardially perfused with ice-cold saline (0.9%). Brains were extracted and hippocampal tissue snap frozen on dry ice prior to

RNA extraction. RNA was extracted from the hippocampus using TRIzol-chloroform (Fisher). RNA was quantified and purity was assessed using a BioTek Synergy HTX Plate Reader with Take3 Microplates and Gen5 Software (Agilent). 1000 ng RNA was used for the reverse transcription reaction using Superscript IV (18091200, Invitrogen) according to the manufacturer's instructions. PCR amplification of cDNA was performed using TaqMan reagents with a QuantStudio 3 detection system (All ThermoFisher: *Actb* – Rn00667869_m1; *Aif1* – Rn00574125_g1; *Bdnf* – Rn02531967_s1; *Cd3* – Rn01417940_m1; *Cd4* – Rn00562286_m1; *Cd8* – Rn00580577_m1; *Cd68* – Rn01495634_g1; *Ciita* – Rn01424725_m1; *Cx3cl1* – Rn00593186_m1; *Cx3cr1* – Rn02134446_s1; *Foxp3* – Rn01525092_m1; *Ifng* – Rn00594078_m1; *Il1b* – Rn00580432_m1; *Il10* – Rn01483988_g1; *Tlr4* – Rn00569848_m1; *Tmem119* – Rn01480631_m1). Gene expression was determined in duplicate with *Actb* as an internal reference gene. All qRT-PCR results were analyzed using the $2^{-\Delta\Delta Ct}$ method (Livak and Schmittgen, 2001) and were normalized across sexes such that the average of the reference group (saline-treated adult males) was set to a value of 1.

2.5. ELISA

Hippocampal tissue was sonicated on ice using a tissue-extraction reagent (FNN0071, Invitrogen) supplemented with protease inhibitor (P2714, Sigma-Aldrich). Homogenates were spun down (14,000 g for 10 min at 4 °C) and supernatant were collected. Centrifugation was repeated one additional time and then samples were stored at −20 °C. Total protein was quantified using a BCA protein assay. An ELISA for rat IL-1β (RLB00, R&D Systems) was run in duplicate according to the manufacturer's instructions. IL-1β concentrations were normalized to total protein.

2.6. Immunohistochemistry, immunofluorescent Imaging, and analysis

Rats received a lethal overdose of Euthasol® Euthanasia Solution (pentobarbital sodium and phenytoin sodium) and then were transcardially perfused with ice-cold 0.1 M phosphate buffered saline (PBS) followed by 4% paraformaldehyde (pH 7.4). Brains were removed, postfixed overnight in 4% paraformaldehyde, cryoprotected in 30% sucrose and then frozen on isopentane on dry ice (approx. 55 °C). Brains were sectioned onto Superfrost Plus slides at 18 μm using a cryostat and stored at 20 °C. For immunohistochemistry, slides were brought to room temperature for 10 min and then underwent a 10 min antigen retrieval step with citrate buffer. Slides were then washed with PBS for 5 min and blocked with 10% normal goat serum for 1 h. Slides were incubated with rabbit anti-rat IBA1 (Wako 019–19741) at 1:1000 overnight and then washed. Slides were incubated for 2 h in secondary (Alexa 568 goat anti-rabbit; 1:500; Invitrogen A11011) and then were washed and coverslipped with vectashield with DAPI. Z stack images were captured at 20X using an Olympus FV3000 confocal microscope (ROI: 0.63×0.63 mm). 3 images per region (CA1, CA3, dentate gyrus) per animal were taken of dorsal hippocampus (bregma −2.8 mm to −3.5 mm), and data reported is the average of these 3 images to generate each data point. Images were then processed and analyzed using Imaris Bitplane to generate semi-automated analysis of IBA1 surface area, IBA1 + cell counts, and microglia soma size.

2.7. Microglia isolation and ex vivo inflammatory challenge

Rats received a lethal overdose of Euthasol® Euthanasia Solution (pentobarbital sodium and phenytoin sodium) and then were transcardially perfused with ice-cold saline (0.9%). Brains were extracted and hippocampal microglia were isolated using a Percoll density gradient as previously described (Fonken et al., 2016b; Frank et al., 2006). Isolated microglia were suspended in DMEM + 10 %FBS and cells counted via hemocytometer with trypan blue exclusion. Cell density was adjusted to 8,000 cells/90 ul and 90 ul plated in a 96-well v-bottom plate. To assess microglia inflammatory responses, cells were challenged with 10 ul lipopolysaccharide (LPS; E. coli serotype 0111:B4; Sigma) at concentrations of 10 ng/mL, 100 ng/mL, and 1000 ng/mL to achieve final concentrations of 1, 10, or 100 ng/mL (respectively) or media alone for 3 h at 37 °C, 5% CO2 (Fonken et al., 2016b; Frank et al., 2010). Following incubation, the plates were centrifuged at 1000 g for 10 min at 4 °C to pellet cells. The supernatant was discarded, cells were washed with 100 ul ice cold PBS and centrifuged at 1000 g for 10 min at 4 °C prior to RNA extraction.

RNA was extracted from isolated microglia using CellsDirect Lysis Buffer (11739010, Invitrogen) following the manufacturer's protocol. The total volume of lysate (11 uL) was used for reverse transcription with Superscript IV (18091200, Invitrogen) according to the manufacturer's instructions. PCR amplification of cDNA was performed using TaqMan reagents with a QuantStudio 3 detection system (All Thermo-Fisher: *Actb* – Rn00667869_m1; *Il1b* – Rn00580432_m1; *Il6* – Rn01410330_m1; *Tnfa* – Rn00562055_m1). Gene expression was determined in duplicate with *Actb* as an internal reference gene. All qRT-PCR results were analyzed using the $2^{-\Delta\Delta Ct}$ method (Livak and Schmittgen, 2001) and werenormalized within each sex such that the average of the reference group (0 ng/mL LPS-treated adults) was set to a value of 1.

2.8. Single nuclei RNA-sequencing

2.8.1. Isolation of nuclei from hippocampal tissue—Single-nuclei samples were obtained from whole hippocampal tissue from 6 adult rats and 6 aged rats (3 rats/sex for each age). Nuclei were obtained from the hippocampus using iodixanol density gradient centrifugation. First, hippocampal tissue was homogenized in a 2 mL Dounce homogenizer with lysis buffer (Nuclei EZ Lysis Buffer, Sigma-Aldrich, NUC101–1KT), 0.2 U/ul RNase inhibitor (NEB, ML314L), and 1x EDTA-free protease inhibitor (Sigma, 5892791001). Samples were then filtered through a 40 μm cell strainer, transferred to a 1.5 mL Eppendorf tube, and centrifuged at 900 g for 5 min at 4 °C. The supernatant was discarded, and the pellet was resuspended with 25% iodixanol that was prepared by combining 437 uL resuspension buffer (1x PBS with 2% BSA and 0.2 U/ul RNase inhibitor) and 312 uL Optiprep density gradient medium (Sigma-Aldrich, D1556). A gradient was then created whereby the 25% iodixanol solution was added on top of 29% iodixanol (569 uL resuspension buffer and 531 uL Optiprep medium). This was then centrifuged at 13,000 g for 30 min at 4 °C with the brake on the centrifuge disengaged. The supernatant was removed, and the pellet was resuspended in 1 mL of resuspension buffer. These samples were centrifuged once more at 600 g for 5 min at 4 °C. The supernatant was removed, and the pellet was resuspended in 100 μl of resuspension buffer. Nuclei were subsequently counted using a hemocytometer, and samples were diluted with resuspension buffer to

achieve a concentration of 1,000 nuclei/μl. These were then submitted to the Genomic Sequencing and Analysis Facility (GSAF) core at The University of Texas at Austin for library preparation and sequencing.

2.8.2. Single-nuclei RNA library preparation and sequencing—Library preparation of samples was performed using an estimated 10,000 nuclei per sample according to the 10x Genomics recommended protocol. Nuclei were counted using a Countess II cell counter, and single-nuclei libraries were prepared using 10x Genomics's Chromium Controller and 3′ single-cell gene expression protocol. Paired-end sequencing was conducted on a NovaSeq 6000 sequencer and an S4 flow cell (200 cycles) with 500 million reads per sample.

2.8.3. Alignment to reference genome—Quality control analyses were first performed on the sequencing data using FastQC. The resulting raw sequencing data was then analyzed using the Cell Ranger software package from 10x Genomics. This allowed for the mapping of reads to cells and for the determination of the number of cells in each sample. The sequencing data was aligned to an annotated rat transcriptome (Ensembl Rnor_6.0) by using the Cell Ranger 5.0 analysis pipeline. To create the custom rat reference file, Cell Ranger's mkref command was used with the Rnor_6.0 GTP and FASTA files. The snRNA FASTQ files were then aligned to the genome by using the count function within Cell Ranger. The "include introns" option was selected to facilitate mapping of unspliced RNAs to the genome.

2.8.4. Cluster analysis and identification—Clusters were analyzed and visualized using the 10x Genomics Loupe Browser. Prior to clustering, nuclei were removed that had fewer than 275 unique molecular identifiers (UMIs) as this may represent low-quality nuclei. Moreover, all mitochondrial genes and reads were excluded from the counts matrix to aid clustering analysis. Following quality control, 133,974 nuclei remained (30,843 adult males, 39,069 aged males, 32,629 adult females, and 31,433 aged females).

Clustering and dimensionality reduction analysis were conducted using uniform manifold approximation and projection (UMAP). 47 graph-based clusters were identified in this manner. To determine the genes that were the most expressed within a cluster, the "Globally Distinguishing" function from the Loupe Browser was used. Then, genes that were significantly and highly expressed within a cluster were analyzed using PanglaoDB, The Human Protein Atlas, and an assortment of studies that incorporated rat genome data to properly identify clusters. Clusters were labeled into one of the 11 major cell types in the hippocampus via marker gene analysis. One cluster containing 10,131 nuclei was not identifiable in this manner and labeled as "Unknown Cells."

2.8.5. Differential gene expression analysis—Bulk data was analyzed using the "Find Features" Seurat function. A pseudobulking approach was used to compare cell type-specific gene expression among the adult and aged rats. Raw RNA counts of each gene from all cells in the clusters were grouped together to produce a pseudobulk gene expression matrix. This data was then normalized, and statistical tests were performed using edgeR in R to identify differentially expressed genes (DEGs). Genes with an adjusted p value under

0.05 were considered differentially expressed. This adjusted p value considers and corrects for multiple comparisons. Marker genes had an adjusted p value under 0.05 and fold change (FC) greater than ±0.25. Gene ontology analyses were performed with the top 500 DEGs using ShinyGO 0.77 to identify enriched KEGG pathways using Ensembl annotations. The top 20 enriched pathways (ranked by False Discovery Rate) are displayed.

2.9. Flow cytometry

Animals were euthanized with Euthasol® and, upon cessation of toe pinch reflex, perfused with ice-cold 0.1 M phosphate buffered saline (PBS). Following perfusion, animals were decapitated and brains removed via the caudal route to preserve meninges integrity in the skull cap.

2.10. Tissue preparation – Brain

Brains were sliced down the midline, with one hemisphere (minus olfactory bulb and cerebellum) taken for flow cytometry. The brain tissue was transferred to an autoclaved 7 mL glass homogenizer filled with 4 mL ice cold sterile RPMI. Tissue was homogenized to obtain a cell suspension. The liquid was passed through a 40 μm cell strainer into a 50 mL tube, along with a rinse of 3 mL RPMI, and centrifuged at 400 g for 5 min at 4 °C to pellet cells. The supernatant was disposed of and cells resuspended in 3 mL 90% Percoll (Fisher 45–001-747) in HBSS. A density gradient was generated by layering over 3 mL 60% Percoll, followed by 4 mL 40% Percoll, then 3 mL HBSS. Samples were then centrifuged at 500 g for 20 min at 4 °C without brake to separate cells (adapted from (Manglani et al., 2018). The top 4 mL of gradient (containing myelin debris) was discarded, and the next 6 mL (containing immune cells) transferred into a fresh tube. 10 mL of HBSS was added to prevent the Percoll gradient from re-forming and cells centrifuged at 400 g for 10 min. The cell pellet was resuspended in 200 μl FACS buffer (PBS with 2% w/v BSA and 2 mM EDTA) and cells were counted using a Neubauer chamber.

2.11. Tissue preparation – Meninges

Meninges were extracted from the skull caps and transferred to 1.5 mL tubes containing 1 mL ice cold RPMI. Tissue was chopped with fine scissors to aid digestion, and enzymes spiked into the RPMI to obtain a concentration of 1 mg/mL collagenase D (Sigma-Aldrich, 11088858001) and 50 μg/mL DNAse 1 (Sigma-Aldrich, 10104159001). Tubes were incubated at 37 °C in a water bath for 30 min, with gentle agitation every 10 min to mix. Following digestion, samples were placed on ice and passed through a 100 μm cell strainer inside a 35 mm petri dish. Tissue was passed through the strainer using a glass pestle and gentle circular motion, with 4 mL of RPMI added to wash the pestle and strainer and collect residual cells. The flow-through was transferred to a 15 mL tube and centrifuged at 400 g, 5 min at 4 °C. The cell pellet was resuspended in 200 μl FACS buffer (PBS with 2% w/v BSA and 2 mM EDTA) and cells were counted using a Countess 3 automated cell counter (ThermoFisher).

2.12. Staining and analysis

All subsequent centrifugation steps were performed at 400 g for 5 min at 4 °C. Cells (total volume or up to a maximum of 1×10^6 cells) were transferred to 96-well V-bottom plate and centrifuged to pellet cells. The supernatant was decanted and cell pellets resuspended in 200 µl PBS followed by a second centrifugation to wash. Supernatant was decanted and cell pellets were then resuspended in 200 µl viability dye (ZombieRed Fixable Dye, Biolegend 423109), diluted 1:1000 in PBS and incubated for 30 min at 4 °C. All incubation steps from this point forward were performed in the dark to preserve fluorescence. Following incubation, the plate was centrifuged, supernatant decanted, and pellets resuspended in 100 µl of antibody mix (see table). Cells were incubated in antibody mix for 30 min at 4 °C. Cells were washed by adding 100 µl of FACS buffer to each well followed by centrifugation. The supernatant was decanted and cells were resuspended in 200 µl of fixation/permeabilization buffer (BD Pharmingen Transcription Factor Buffer Set, 562574). Cells were incubated in the fix/perm buffer for 30 min at 4 °C, then centrifuged. The supernatant was decanted and cells resuspended in 200 µl permeabilization/wash buffer (BD Pharmingen Transcription Factor Buffer Set, 562574) to wash. The plate was centrifuged to pellet cells, supernatant decanted, and cell pellets resuspended in 200 µl FACS buffer for overnight storage at 4 °C prior to intracellular staining. Plates were centrifuged and cells resuspended in 100 µl intracellular stain (anti-FoxP3; clone 150D, Biolegend 320007, 1:100 in perm buffer) for 30 min at 4 °C, washed with the addition of 100 µl permeabilization/wash buffer, centrifuged, resuspended in 200 µl permeabilization/wash buffer as a second wash, centrifuged, and finally resuspended in 200 µl FACS buffer prior to analysis. To quantify cells, 20 µl counting beads (ThermoFisher C36950) were added to each sample prior to running. Samples were acquired using a BD Fortessa (core facility) and FACSDiva v6.1.3. Rainbow beads (BD Biosciences 559123) were used to standardize acquisition parameters between 3 runs. Sample analysis was performed using FACSDiva v6.1.3 and FlowJo v10.8.1.

Target	Fluor	Clone	Supplier	Catalogue Number	Dilution
CD4	V450	OX-35	BD Bioscience	561,579	200
CD44	BV510	OX-49	Biolegend	203,906	100
CD3	BV605	1F4	BD Bioscience	563,949	100
CD25	AlexaFluor488	OX-39	BD Bioscience	742,753	100
CD62L	PerCP	OX-85	Biolegend	202,914	100
CD11b/c	PE-Cy7	OX-42	BD Bioscience	562,222	100
CD8	APC	G28	Biolegend	200,610	200
CD45	AlexaFluor700	OX-1	Biolegend	202,218	100

2.13. Ovariectomy

23-month-old female rats were anesthetized with isoflurane anesthesia and received a local 0.5% lidocaine injection (7 mg/kg, s.c.). Buprenorphine (0.05 mg/kg, s.c.) was administered directly prior to surgery as well as at 12 h intervals until least 48 h post-surgery. Rats were shaved and the surgical area was prepared with ethanol and betadine. A single midline

incision was made through the skin along the dorsum (approx. 2 cm) directly below the level of the ribcage. The muscle wall was opened one side at a time (approx. 1 cm). The ovarian fat pad was located and withdrawn, the uterine horn was clamped directly below the ovary and the ovary removed. The muscle wall was sutured with sterile absorbable sutures and the skin was closed with wound clips. The area was treated with Neosporin and wound clips were removed by 14 days post-surgery. Sham rats underwent the same surgical manipulations except ovaries were left intact. Rats were allowed at least one month from surgery prior to further experimental manipulations.

2.14. Experimental design and statistical tests

Group sizes for experiments were based on prior published work (Fonken et al., 2016a; Fonken et al., 2018a; Fonken et al., 2018b) and separate cohorts were used for behavioral and molecular readouts. Data were analyzed using GraphPad Prism 9. Data presented in the figures are expressed as mean ± standard error of the mean (SEM). Two- and three-way ANOVA were used to analyze experiments with two and three independent variables, respectively, with post hoc tests performed if main effects were observed. The p values for post hoc tests were adjusted for multiple comparisons using Tukey's or Sidak's correction. Full results of statistical tests performed are given in Supplemental Tables. The α level for all tests was set at 0.05, numbers of animals used are detailed in each figure legend.

3. Results

3.1. Aged male but not aged female rats exhibit prolonged cognitive deficits at 4 days following LPS

Previous work indicates that aged male rats exhibit prolonged drops in cognitive function following diverse peripheral immune challenges (e.g., surgery, *E. coli*) (Barrientos et al., 2009; Barrientos et al., 2012; Fonken et al., 2016a). Here we examined whether aged female rats exhibited comparable impairments in cognitive function following an intraperitoneal LPS injection (40 μg LPS). 48 h following LPS or saline, adult and aged male and female rats underwent fear conditioning and then were tested for freezing behavior 48 h later (freezing tested at 96 h post-LPS; see Fig. 1A for experimental outline). Aged male but not female rats that received LPS exhibited reduced freezing behavior, indicating impaired learning and memory in the fear conditioning task (sex × age × LPS: $F_{1,59} = 4.501$, $p < 0.05$; Fig. 1B, Supplemental Table S1). Indeed, aged male rats that received LPS reduced freezing behavior as compared to aged male saline rats, adult male LPS rats, and aged female LPS rats ($p < 0.05$ in all cases). Rats were also assayed for freezing behavior in a control context (novel chamber): overall freezing was lower in the control context but no differences were observed between groups ($p > 0.1$, Supplemental Fig. S1B, Supplemental Table S2). In order to determine whether the lack of cognitive impairment was a dose-specific phenomenon, two additional LPS doses were tested in aged female rats. Similar to the 40 μg LPS dose, aged female rats did not exhibit cognitive impairments in a fear conditioning task when trained 48 h following a 30 μg or 60 μg dose of LPS ($p > 0.1$ in all cases) (Supplemental Fig. S1C, Supplemental Table S2). Thus, aged males, but not females, display protracted cognitive deficits after peripheral immune activation.

3.2. Aged male but not aged female rats exhibit increases in hippocampal IL-1β 48 h following LPS

Prior work indicates that increases in IL-1β are critical for prolonged cognitive deficits in aged male rats following peripheral immune challenges (Barrientos et al., 2009; Barrientos et al., 2012). Thus, we next evaluated IL-1β gene and protein expression in the hippocampus 48 h following i.p. LPS injection. *Il1b* gene expression was elevated in the hippocampus of aged male but not aged female rats 48 h following LPS (age × sex × LPS: $F_{1,23}$ = 13.32, $p < 0.05$) (Fig. 2A, Supplemental Table S3). Hippocampal *Il1b* in aged male LPS rats significantly differed from all groups in which a comparison is appropriate, including aged female LPS rats, adult male LPS rats, and aged male saline rats ($p < 0.05$ in all cases). IL-1β protein expression followed the same pattern: aged male rats that received LPS exhibited elevated hippocampal IL-1β protein expression as compared to conspecifics (age × sex × LPS: $F_{1,24}$ = 17.000 and post hoc comparisons $p < 0.05$; Fig. 2B, Supplemental Table S3).

We subsequently performed a time course evaluating hippocampal *Il1b* gene expression at baseline and 6, 24, and 48 h following LPS. *Il1b* is persistently elevated in aged male hippocampi following LPS challenge (sex × age: $F_{1,46}$ = 4.24, LPS: $F_{3,46}$ = 16.45, and post hoc comparisons, $p < 0.05$) (Fig. 2C, Supplemental Table S3). Interestingly, increases in hippocampal *Il1b* in aged male rats were accompanied by reduced hippocampal *Bdnf* gene expression in aged males (sex × age: $F_{1,48}$ = 7.08, LPS: $F_{3,48}$ = 5.84, and post hoc comparisons, $p < 0.05$) (Fig. 2D, Supplemental Table S3).

3.3. Hippocampal microglia exhibit divergent morphology following LPS administration in aged male rats compared to aged females

Microglia are the dominant source of cytokines in the CNS and they exhibit changes in morphology and cytokine production with aging. Therefore, we performed immunohistochemistry analysis of hippocampal subfields to establish whether sex differences in this age-associated neuroinflammatory potentiation were underscored by changes in microglial morphology. Multiple aspects of hippocampal $IBA1^+$ microglia shape and number were altered with aging and sex (Fig. 3 and Supplemental Tables S4 and S5). In the dentate gyrus (Fig. 3A, Supplemental Table S5), there were increases in the number of $IBA1^+$ microglia per region of interest (0.63×0.63 mm) with age ($F_{1,21}$ = 10.53, $p < 0.05$) (Fig. 3B, Supplemental Table S5). $IBA1^+$ microglia staining volume was also differentially altered by LPS treatment in males versus females (sex × LPS: $F_{1,21}$ = 13.14, $p < 0.05$): this change in staining volume was driven by an increase in volume in aged males treated with LPS ($p < 0.05$ compared with saline-treated aged males) (Fig. 3C, Supplemental Table S5). Importantly, this sex × LPS interaction in $IBA1^+$ staining volume occurred throughout the hippocampal subfields analyzed including the dentate gyrus, CA1, and CA3 (Supplemental Tables S4 and S5). Interestingly, females exhibited a reduction in $IBA1^+$ microglia cell soma size compared to males (sex: $F_{1,23}$ = 14.41, $p < 0.05$), irrespective of age (Fig. 3D, Supplemental Table S5). These results suggest that sex-specific shifts in microglial priming may drive the heightened pro-inflammatory response in aged male but not female rats.

3.4. Microglia isolated from the hippocampus of aged male but not female rats exhibit potentiated inflammatory responses

Next, microglia were isolated from the adult and aged hippocampus of male and female rats to determine whether sex differences in microglial priming contribute to the altered neuroinflammatory response with aging (Fig. 4A). We observed significant sex × age interactions for all cytokines analyzed (*Il1b*: $F_{1,76} = 5.067$; *Il6*: $F_{1,72} = 7.648$; *Tnfa*: $F_{1,72} = 12.38$, all $p < 0.05$) (Supplemental Table S6). Consistent with prior work (Fonken et al., 2016b; Frank et al., 2010), microglia isolated from the aged male hippocampus exhibited a potentiated pro-inflammatory response to LPS challenge (*Il1b*: $F_{1,36} = 9.930$; *Il6*: $F_{1,32} = 7.159$; *Tnfa*: $F_{1,36} = 5.303$, all $p < 0.05$). In contrast, microglia isolated from the aged female hippocampus did not exhibit potentiated responses to LPS (*Il1b*: $F_{1,40} = 0.4267$; *Il6*: $F_{1,40} = 3.124$, both $p > 0.05$) and expression of *Tnfa* was lower in the aged group than in the young group ($F_{1,36} = 7.090$, $p < 0.05$) (Fig. 4B – D, Supplemental Table S6). These data suggest that microglia in the aged female rat brain may not take on the same “primed” phenotype that has been described in aged male microglia.

3.5. The aged male and female hippocampus have divergent neuroinflammatory gene profiles

To further determine how sex differences in the inflammatory milieu of the hippocampus occur in aged male versus female rats, we assessed baseline expression of microglia-related genes *Aif1* (which encodes the IBA1 protein)*, Tmem119, Cd68, Ciita, Tlr4, Cx3cl1* and *Cx3cr1* (Fig. 5A, Supplemental Table S7). These genes were selected to give a broad profile of homeostatic and innate immune signaling. Several immune markers were elevated in the aged hippocampi including *Aif1* (age: $F_{1,12} = 11.25$), *Cd68* (age: F: $_{1,12} = 32.52$), *Ciita* (age: F: $_{1,12} = 49.02$), *Tlr4* (age: $F_{1,12} = 19.08$), and *Tmem119* (age: $F_{1,12} = 4.755$), all $p < 0.05$. Interestingly, a few of these genes were also modestly upregulated in the female as compared to the male hippocampus including *Aif1* (sex: $F_{1,12} = 10.55$), *Tlr4* (sex: $F_{1,12} = 5.101$), and *Tmem119* (sex: $F_{1,12} = 6.693$), all $p < 0.05$. Both *Cx3cl1* and its cognate receptor *Cx3cr1* showed a significant interaction (*Cx3cl1* age × sex: $F_{1,12} = 6.126$; *Cx3cr1* age × sex: $F_{1,12} = 5.259$, both $p < 0.05$), with increased expression in aged females relative to aged males (both $p < 0.05$).The Cx3cl1-Cx3cr1 pathway regulates microglial homeostasis (Limatola and Ransohoff, 2014), dampens inflammation, and promotes chemotaxis of T cells (Rayasam et al., 2018), so this may indicate a sex-specific shift in immune balance in the aged hippocampi.

As T cells also regulate age-associated cognitive changes, we profiled baseline expression of T cell-related markers *Cd3, Cd4, Cd8, Il10, Ifng,* and *Foxp3* (Fig. 5B, Supplemental Table S7). The pan-T cell marker *Cd3* was strikingly elevated in the aged female but not aged male hippocampus (age × sex: $F_{1,12} = 11.17$, $p < 0.05$). The T helper cell-specific marker *Cd4* was increased in both aged groups with no sex differences (age: $F_{1,12} = 110.8$, $p < 0.05$), whereas *Cd8* showed a significant interaction with enhanced expression in aged female hippocampi (age × sex: $F_{1,12} = 5.259$, $p < 0.05$), matching the pattern of *Cd3* expression. No significant differences were found in expression of the canonical regulatory T cell (Treg) marker *Foxp3*. We also observed a reduction in the Treg- and Th2- associated cytokine *Il10* with age (age: $F_{1,12} = 8.536$, $p < 0.05$). In contrast, the Th1-associated cytokine *Ifng* was not affected by

age, but was significantly elevated in female compared to male hippocampus (sex: $F_{1,12} = 5.457$, $p < 0.05$). Taken together, these results indicate an age-dependent increase in T helper ($CD4^+$) signaling, which may promote inflammation in aged hippocampi; and a sex-specific enhancement of cytotoxic ($CD8^+$) T cell signaling in aged females, which may facilitate cellular immunity.

To assess broader changes in the rat hippocampal transcriptome with age and/or sex, we performed single nuclei sequencing as an unbiased screen (Fig. 6A). We observed 5,765 differentially expressed genes (DEGs) in male hippocampi (adult vs. aged) and 2,686 DEGs in female hippocampi (adult vs. aged). Of these DEGs, only 1,537 were shared between the sexes, indicating substantial sex-specific effects of aging on the hippocampal transcriptome (Fig. 6B). Analysis of the bulk sequencing component revealed that males showed significant upregulation of genes associated with pathways of neurodegeneration and neurodegenerative diseases such as Parkinson's, Huntington's, and Alzheimer's diseases (e.g., *Calm1, Sod1, Tubb4a, Vdac3*), and metabolic pathways (e.g., *Ckb, Guk1, Mdh2*), whereas females showed significant upregulation only in pathways associated with Th1 and Th2 cell differentiation (e.g., *Notch2, RT1-Ba, RT1-Db1, Stat5b*) and toxoplasmosis (e.g., *Birc7, Lamc1, Stat3*) (Fig. 6C). In contrast, females showed significant downregulation of those same neurodegenerative pathways that were upregulated in males (e.g., *Calm1,* along with *Apoe*, *Mcu*, and *Snca*), whereas males showed significant downregulation of neurotrophin signaling pathway (e.g., *Camk2d, Plcg2, Shc3*) and apoptosis (e. g., *Bcl2, Ma. pk8, Ma. pk10*). Both sexes showed downregulation of pathways associated with long-term potentiation (e.g., *Adcy1/8, Grin2b, Ppp3ca/cc*) and axon guidance (e.g., *Dcc, Robo1, Sema6a, Srgap1*). These results suggest that aged males exhibit a metabolic shift in the brain, which may potentiate responses to inflammatory stimuli and neurodegeneration, whereas females present a less neurodegenerative profile which may support maintenance of cognitive function.

We further clustered cells into populations via UMAP to facilitate more detailed investigation of hippocampal microglia (Fig. 6D). As expected, multiple populations of neuronal and glial subtypes were detected, along with a population of immune cells which broadly clustered with microglia and showed enrichment for immune-related genes (*Arhgap15, Dock8, Lyn, Ikzf1, Slco2b1*) but did not express classical microglia signature genes (i.e., *Aif1*, *Cd68*, *Cx3cr1*, *P2ry12* and *Cd200r1*). Quantification of differentially-expressed genes in each cell population showed critical differences in how male and female brains respond to aging at the transcriptional level (Fig. 6E and F, Supplemental Fig. S2). Surprisingly, we did not observe significant changes in transcriptomic profiles of male microglia with aging, whereas female microglia showed significant downregulation of transthyretin (*Ttr*) and upregulation of inflammatory markers including *Cd74, Gpr34*, and MHCII components (*RT1-Ba, RT1-Db1, RT1-Bb, RT1-Da*) (Fig. 6F). These results indicate a sex-specific change in microglial function with aging, which appears more conducive to antigen presentation in aged females than aged males.

Analysis of additional neuroimmune populations revealed distinct cell-specific profiles of transcriptomic changes, indicating that additional cell populations modulate sex-specific changes in brain aging (Fig. 6E, Supplemental Fig. S2). Male astrocytes showed 10-fold

more DEGs than female astrocytes, whereas female oligodendrocytes showed 500-fold more DEGs than male oligodendrocytes. Numbers of DEGs in the immune cell cluster were of the same order of magnitude in both males and females (32 and 18 DEGs, respectively).

3.6. Sex differences in CNS immune cell populations

To assess whether the sex differences seen in age-dependent cognitive changes and neuroinflammatory gene expression profiles were indicative of underlying changes to immune cell presence in the CNS, we performed flow cytometry analysis of brain and meninges 48 h following LPS challenge (or saline control). Cell populations are illustrated as % of live cells recorded (see Supplemental Fig. S3A and Supplemental Fig. S3B for gating strategies).

There was an increase in T cells within the aged brain, and in females (age: $F_{1,57} = 28.10$; sex: $F_{1,57} = 4.10$, both $p < 0.05$), whereas LPS treatment had no significant effects (Fig. 7A, Supplemental Table S8). Aged females exhibited higher numbers of T cells than young females at baseline (saline treatment) ($p < 0.05$). This pattern was similar in all T cell subsets analyzed. For $CD8^+$ T cells, there were increases in $CD8^+$ T cells specifically in aged females as compared to young females (age × sex: $F_{1,57} = 4.03$, $p < 0.05$) (Fig. 7B, Supplemental Table S8). For $CD4^+$ T cells, there were also increases with age ($F_{1,57} = 19.14$, $p < 0.05$), and again more $CD4^+$ T cells in aged females than young females at baseline ($p < 0.05$) (Fig. 7C, Supplemental Table S8). The population of $CD4^+$ T effector cells (Teffs: $CD4^+CD25^+FoxP3^-$), was specifically increased in aged females but not males (age × sex: $F_{1,57} = 5.41$, $p < 0.05$) (Fig. 7C, Supplemental Table S8). Finally, there was a significant increase in the numbers of Tregs ($CD4^+CD25^+FoxP3^+$) with age ($F_{1,57} = 4.30$, $p < 0.05$) (Fig. 7C, Supplemental Table S8). These results indicate that there is a significant increase in multiple populations of T cells into the brain with aging, but that treatment with LPS does not induce further recruitment at this time point. Given that both effector and regulatory populations were increased with aging, this appears to be a global shift in the presence of T cells in the parenchyma, resulting in both pro- (effector cells) and anti-inflammatory (regulatory cells) effects.

Given that the meninges also act as a local immune niche for the brain, we examined T cell populations in this compartment. T cells were increased in the meninges of aged females; however, the increase in T cells in females was reversed by LPS treatment (age × LPS: $F_{1,58} = 13.35$, $p < 0.05$; trend for age × sex: $F_{1,58} = 3.546$, $p = 0.06$). Specifically, there were increases in the % of T cells in aged saline-treated females compared with adult saline-treated females, and aged LPS-treated females (both $p < 0.05$) (Fig. 7D, Supplemental Table S8). This suggests an increase in the presence of T cells in the meninges of aged females at baseline, which may be activated upon inflammatory stimulation.

Probing each T cell subset further revealed consistent increases in subpopulations of T cells in aged females in the absence of immune stimulation. Indeed, the % of $CD8^+$ T cells ($CD3^+CD8^+$) was increased in aged saline treated females (age × sex: $F_{1,58} = 5.27$; age × LPS: $F_{1,58} = 7.44$, both $p < 0.05$) compared to adult saline-treated females and aged saline-treated males (both $p < 0.05$) (Fig. 7E, Supplemental Table S8). Similarly, there were increases in the % of $CD4^+$ T cells ($CD3^+CD4^+$) (age × sex: $F_{1,58} = 4.38$; age × LPS: $F_{1,58}$

= 6.54, both $p < 0.05$) in aged saline-treated females. In particular, there was an increase in the % of $CD4^+$ T cells in aged saline-treated females compared with adult saline-treated females, aged saline-treated males, and aged LPS-treated females (all $p < 0.05$) (Fig. 7F, Supplemental Table S8). $CD4^+$ T effector cells (Teffs: $CD4^+CD25^+FoxP3^-$) were similarly increased in aged saline-treated females (age × sex: $F_{1,58} = 4.639$; age × LPS: $F_{1,58} = 10.00$, both $p < 0.05$) with an increase in the % of Teffs in aged females compared with adult females and aged males (both $p < 0.05$) (Fig. 7F, Supplemental Table S8). There were also increases in Tregs ($CD4^+CD25^+FoxP3^+$) (age × LPS: $F_{1,58} = 8.17$, $p < 0.05$), with a specific increase in aged saline-treated females compared to adult saline-treated females ($p < 0.05$) (Fig. 7F, Supplemental Table S8). Taken together, these results suggest that a significant shift in immune profile occurs in the meninges of aged females, with increases in all T cell subsets (both pro- and anti-inflammatory) observed at baseline.

3.7. Ovariectomy in aged female rats did not increase neuroinflammatory responses

Ovarian hormones such as estrogens are known to have anti-inflammatory and neuroprotective effects (Arevalo et al., 2015). Indeed, many neurodegenerative disorders have an onset post-menopause in humans (Li et al., 2002) and aging is a major risk factor for neurodegenerative diseases (Hou et al., 2019). Earlier age at menopause is linked with earlier onset of Alzheimer's disease (Corbo et al., 2011) and increased tau deposition in the brain (Coughlan et al., 2023). Importantly, rats do not undergo menopause with the associated loss of estrogen and progesterone that occurs in humans, instead exhibiting estropause and a persistent estrous state (Koebele and Bimonte-Nelson, 2016). Thus, to test whether the neuroinflammatory response seen in aged females was mediated by ovarian hormones, we performed ovariectomy (OVX) in aged rats to remove the major source of sex hormones in females. At least one month following surgery, we tested OVX and sham animals for behavioral and neuroinflammatory responses 48 h following LPS injection. There was no effect of OVX or LPS on freezing behavior in the fear conditioning paradigm (both $p > 0.1$; Fig. 8A, Supplemental Table S9). As in our intact cohort (Fig. 1B), sham-operated females did not show a significant impairment of freezing behavior following LPS administration. OVX females also did not show an impairment of freezing behavior, although this group showed greater variability in their response.

In a second cohort of rats, we analyzed expression of *Il1b* in the hippocampus 48 h following LPS or saline vehicle (Fig. 8B, Supplemental Table S9). Although there was no interaction effect of LPS and OVX on *Il1b* expression, there was a trend towards increased expression following LPS ($F_{1,16} = 3.47$, $p = 0.08$) and in OVX females ($F_{1,16} = 3.56$, $p = 0.08$). In a third cohort of rats, microglia were isolated and stimulated *ex vivo* with LPS. OVX did not alter *ex vivo* responses to LPS, suggesting that ovarian hormones were not masking an age-associated priming response in females ($p > 0.1$) (Fig. 8C, Supplemental Table S9). Taken together, these results indicate that while OVX did appear to increase variability in inflammatory and behavioral outcomes, it did not induce the potentiated neuroinflammatory state that occurs in aged male rats.

4. Discussion

Aging is associated with amplified neuroinflammatory responses that can contribute to cognitive deficits. The majority of work investigating age-associated neuroinflammatory priming has been conducted in male rodents. There are sex differences in “inflammaging” (Gubbels Bupp et al., 2018) and age-associated risk for cognitive decline (Levine et al., 2021) which led us to investigate sex differences in neuroinflammatory and cognitive changes with age. Overall, we demonstrate that female rats are more resilient to age-associated inflammatory priming and do not exhibit enhanced neuroinflammatory responses to peripheral immune challenge. At the behavioral level, this was manifest as a resistance to inflammation-induced impairment in hippocampal-dependent learning and memory in aged males, but not aged females. These sex-specific effects on behavior were correlated with enhanced neuroinflammatory signaling within the aged male brain, and age- and sex-specific changes to the neuroinflammatory environment as determined by transcriptomic and flow cytometry analyses. Female-specific resistance to age-associated inflammatory priming did not appear dependent on ongoing ovarian hormone signaling, pointing towards additional regulation of sex-specific resilience to aging.

In agreement with prior work, aged male rats exhibited persistent impairments in memory in a fear conditioning paradigm following immune stimulation (Barrientos et al., 2006; Fonken et al., 2016b; Barrientos et al., 2009; Fonken et al., 2018a). In contrast, aged female rats did not exhibit impairments compared to young females. These data indicate that aged female rats show an enhanced resilience to inflammation-induced memory impairments compared to aged males. This finding is consistent with recent work highlighting the differences between hippocampus-dependent memory impairment in male and female rats, wherein high fat diet had no effect on contextual fear conditioning in females (Muscat et al., 2023) but has been reported in males (Spencer et al., 2017). Aging is typically associated with cognitive decline and increased inflammation, but a significant portion of the preclinical literature has focused on solely male cohorts, resulting in a biased account of age-associated behavioral, cellular, and molecular changes. In contrast, cognitive decline in humans is known to show sex-specific patterns, with women showing enhanced cognitive reserve compared to men (Levine et al., 2021) but increased prevalence of Alzheimer’s disease (2022 Alzheimer’s disease facts and figures, 2022). The resistance of aged female rodents to inflammation-induced hippocampus-dependent cognitive changes raises the question of how neuroinflammatory signals are modified in an age- and sex-specific manner to regulate behavior.

At the cellular and molecular levels, we focused on two major contributors to neuroinflammatory pathology: microglia and T cells. As with our previous data (Fonken et al., 2016b), we observed that microglia from aged males showed higher production of pro-inflammatory molecules *Il1b*, *Il6*, and *Tnfa* than microglia from adult males following *ex vivo* stimulation. However, microglia from aged females showed no such inflammatory priming, producing less *Tnfa* than cells from adult females, indicating a fundamental sex difference in this key neuroimmune cell population. This effect also occurred in gene expression in whole hippocampus following *in vivo* inflammatory challenge, and directly correlates with the pronounced behavioral changes observed in aged males but not aged

females. Age-related and sex-related differences in microglial morphology were apparent in multiple regions of the hippocampus, including decreased soma volume in females and increased cell numbers with age. The differences we observe illustrate a tendency for aged male microglia to possess a larger soma, which is associated with a more inflamed/reactive cell state, rather than a smaller soma relative to overall IBA1+ coverage seen in females, which indicates a more surveillant state (Davis et al., 2017). Whilst IBA1 staining is a limited readout of microglial morphology due to the presence of IBA1^{-} microglia and IBA1 expression by infiltrating myeloid cells (Lier et al., 2021), these data, combined with our *ex vivo* stimulation of isolated microglia, suggest that male microglia are more susceptible to age-related inflammatory priming, whereas female microglia are relatively resistant.

The morphological changes we report here are consistent with sex-specific morphological differences in a mouse model of Alzheimer's disease and in post mortem tissue from patients, in which microglia from males exhibit a larger soma size and more amoeboid shape (Guillot-Sestier et al., 2021). Other studies, not stratified by sex, demonstrate that microglial morphology is significantly changed in neurological disease states such as Alzheimer's disease and other dementias, with a greater proportion of dystrophic microglia (Bachstetter et al., 2015) and reduced arborization (Davies et al., 2017) present in diseased brains relative to age-matched controls.

An underlying sex difference in microglia aging may be a key mediator of sex differences in the pathogenesis of neurodegenerative diseases, as the enhanced abundance of amoeboid microglia in male Alzheimer's disease patients is associated with reduced amyloid burden (Guillot-Sestier et al., 2021). Indeed, an initial resistance to inflammatory stimulation in females would preserve cognition in the short-term, but may facilitate deposition of harmful materials which, when accumulated over time, become detrimental and lead to more severe impairments with disease progression. This sex-specific difference in inflammatory priming may therefore contribute to the faster cognitive decline observed in women (Levine et al., 2021), leading to worse outcomes overall in aged females despite a greater initial cognitive reserve.

Analysis of hippocampal gene expression at baseline (i.e., without any inflammatory stimulus) further highlighted age- and sex-specific changes in the inflammatory milieu of this brain region. Prior work in mice has implicated impairments in fractalkine signaling in age-related neuroinflammatory priming, as *Cx3cr1*$^{-/-}$ mice exhibit persistent microglial activation and extended social withdrawal following inflammatory challenge (Corona et al., 2010). Here, we observed increased expression of both *Cx3cr1* and its cognate ligand, *Cx3cl1*, in the hippocampus of aged female rats relative to aged males, which may reflect the involvement of this pathway in the resilience of aged females to hippocampal inflammation and impairment in hippocampal-dependent memory formation. Interestingly, sexual dimorphism in Cx3cr1-Cx3cl1 signaling underlies differences in susceptibility to diet-induced obesity between male and female mice: males fed high-fat diet showed increased microglial activation along with reduced expression of both receptor and ligand, whilst females maintained Cx3cr1-Cx3cl1 expression levels and were resistant to the effects of high fat diet on microglial activation (Dorfman et al., 2017).

Alongside sex differences in age-related behavioral changes and cytokine production, we report changes to T cell physiology within the brain. In particular, striking increases in gene expression of the pan-T cell marker *Cd3* were apparent in hippocampi from aged females relative to any other group, which suggests an increased T cell presence in this tissue in aged females. We observed a parallel increase in the expression of cytotoxic T cell marker *Cd8* in aged female hippocampi, indicating that cellular immunity, in particular, may be enhanced in the hippocampi of aged females. An increase in $CD8^+$ T cells is observed in aged brains, and these adaptive immune cells modulate both microglial and oligodendrocyte function (Kaya et al., 2022). Thus, sex-specific changes in adaptive immune signaling may contribute to alterations in brain-resident immune populations (as observed in our transcriptomic analyses). Although an accumulation of $CD8^+$ T cells is linked with white matter decay (Liston and Yshii, 2023) and cognitive impairment (Reagin and Funk, 2022), our data do not indicate that these cells are detrimental to hippocampal-dependent memory in aged females at this stage. It remains to be determined whether greater cognitive impairment manifests in females at later stages, or whether the female brain possesses mechanisms to adapt to an age-associated influx in adaptive immune signaling.

Single-cell transcriptomic analysis further indicated a sex-specific shift in hippocampal gene expression, with males showing upregulation of metabolic and neurodegenerative pathways and females showing downregulation of neurodegenerative pathways at the bulk level. Analysis of the microglia cluster also highlighted a sex-specific change in the neuroimmune landscape of these key neuroimmune cells. Surprisingly, we did not detect any significantly altered genes between adult and aged male microglia. In contrast, we observed that aged female microglia exhibited a reduction in transthyretin (*Ttr*) expression and upregulation of several inflammatory markers compared to adult females. For example, aged females exhibited increases in *Gpr34*, a GPCR member of the $P2Y_{12}$-like group. This gene is also increased in hippocampal and cortical microglia from the TASTPM mouse model of Alzheimer's disease (Bonham et al., 2019). In mice, GPR34 signaling regulates inflammation (Sayo et al., 2019) and phagocytic activity of microglia (Preissler et al., 2015), suggesting that increases in the expression of *Gpr34* may modulate inflammatory and phagocytic function in aged females. We also observed increases in *Cd74* and MHCII-related genes in aged female rats. Overexpression of *Cd74* and *Gpr34* were previously identified in aged female hippocampi as part of an 11-gene signature of inflammatory processes which are overexpressed across species with aging (Pardo et al., 2017). Although not included in the cross-species aging signature, the authors also detected increased *RT1-Ba* and *RT1-Db1* in aged rats; MHCII-related genes which were also identified as overexpressed in our aged female microglia. Interestingly, age-associated transcriptional changes in the MHCII pathway have previously been reported in the cortex of male rats, with an increase at 12 months followed by a decrease at 28 months when compared to 6-month-old controls (Wood et al., 2013). As our aged cohort is 24 months old, we may be capturing a time point of enhanced inflammatory priming prior to eventual dysregulation of antigen presentation by 28 months (as studied by Wood et al.) and impaired capacity to respond to immune challenges. It is important to note, however, that microglia show substantial heterogeneity which also changes across the lifespan (Hammond et al., 2019; Stratoulias et al., 2019). New subsets of microglia have been identified in aging and

pathology, including proinflammatory “dark microglia” (Bisht et al., 2016) and lipid-droplet accumulating microglia (Marschallinger et al., 2020), which may introduce additional heterogeneity into our microglia cluster and confound significant changes in gene expression of microglia sub-populations within our overall cluster due to limited resolution of different microglia subsets. Although Hammond et al. found a minimal effect of sex on microglial subpopulations, their analysis was restricted to much younger ages (e14.5, p4/5, and p100 in mice) and was not included as a variable at later timepoints (Hammond et al., 2019). We hypothesize that sex-specific changes in microglial heterogeneity may also occur with age, which may influence the transcriptional changes (or lack thereof) seen in the present study.

The gene expression data raised the question of whether T cell numbers within the brain were modified in an age- and sex- specific manner. To address this, we performed flow cytometry on brain tissue and quantified immune cell populations. We observed an increase in the proportion of T cells in the brain with aging, in line with previous data showing T cell infiltration of aged brains (Dulken et al., 2019) and in inflammatory scenarios (Xu et al., 2010). The increase in T cells was apparent in multiple subsets ($CD4^+$, $CD8^+$, $CD4^+CD25^+FoxP3^-$, and $CD4^+CD25^+FoxP3^-$), indicating an increase in cell infiltration (e.g., via active recruitment or increased blood-brain barrier permeability) or expansion of T cells in the aged rat brain. T cell populations were also increased in the brain of female as compared to male rats. Indeed, increases in T cell populations with aging appeared particularly driven by aged female rats with respect to certain populations such as the $CD8^+$ and $CD4^+CD25^+FoxP3^-$ populations (sex × aging interaction; however, the high variability reduced statistical power to detect changes with pairwise comparisons).

T cell recruitment to aged brains is facilitated by microglia through chemokine signaling pathways (Zhang et al., 2022), and the CX3CR1-CX3CL1 axis is involved in T cell recruitment in inflammatory scenarios (Broux et al., 2012). We identified both *Cx3cl1* and *Cx3cr1* as upregulated in aged female hippocampi compared to aged males at baseline, which may mediate the age- and sex- differences observed in T cell numbers in brain hemispheres. Whilst excessive immune cell accumulation in the brain is indicative of an inflamed environment and T cell infiltration is implicated in brain aging (Kaya et al., 2022), T cell depletion leads to cognitive impairment (Kipnis et al., 2004) and Tregs play an important role in attenuation of neuroinflammatory pathology (Liston et al., 2022), highlighting the need for further characterization of immune cell populations and functions in aged brains. We hypothesize that the microglia-T cell interactions in aged females are more immunosuppressive and tolerogenic compared to that of aged males, and that this mediates sex-specific changes in the behavioral consequences of inflammatory stimulation.

Alongside flow cytometry of brain samples, we also analyzed meninges from the same animals to investigate changes to the inflammatory environment at this key neuroimmune interface. Here, we observed interactions between age, sex, and inflammation such that $CD4^+$, $CD8^+$, and $CD4^+CD25^+FoxP3^-$ T cells were increased in aged females compared to aged males at baseline, and the $CD4^+$ population was reduced in aged females following LPS administration. Thus, the meninges in aged females likely shifts towards a potentiated state housing T cells that may be activated upon peripheral immune stimulation and suggests a greater capacity for T cell-mediated immune signaling in female rats and with age.

Finally, we directly manipulated sex hormone signaling to assess the potential role of ovarian hormones in attenuating neuroinflammation and protecting from cognitive decline. Previous studies identified protective effects of ovarian hormones on neuroinflammatory responses (Benedusi et al., 2012), including an increase in hippocampal expression of pro-inflammatory cytokines and exacerbated sickness responses to inflammatory stimulation in ovariectomized mice (Sanchez et al., 2023). Ovariectomized rats also show enhanced expression of inflammatory cytokines in the dentate gyrus, which is attenuated by estrogen replacement (Kireev et al., 2014). We thus performed the inflammatory challenge in a cohort of aged females who had undergone ovariectomy or sham surgery; ovariectomized females were also resistant to LPS-induced memory deficits, although there was greater variability in the display of freezing behavior in the LPS-treated OVX group. In the hippocampus, there was a trend towards increased inflammation following LPS in OVX rats, but OVX did not elicit inflammatory potentiation of isolated microglia, suggesting that additional cell populations play a role in the broader hippocampal response (e.g., *Il1b* production by monocytes/macrophages, or potentiation of microglial *Il1b* production *in situ* by other cells). These results indicate that ovarian hormones are not the major factor driving this sex-specific resilience to inflammatory signaling, and further investigation is warranted to elucidate the mechanisms behind the reduced susceptibility of aged females to neuroinflammatory priming with age.

In conclusion, here we show that aged male, but not female rats exhibit LPS-elicited deficits in hippocampus-dependent memory. These sex differences in behavior show striking parallels with dimorphism in microglial priming – aged male microglia have morphological, gene signature, and functional outputs suggestive of microglial priming, whereas aged female microglia have a less primed phenotype. Cell sequencing and flow cytometry data showed that aged female brains and meninges contained more T cells, implying that the female CNS may have a bias towards an adaptive response. OVX in aged females did not unmask hippocampal inflammation nor microglial priming. Together, our data point towards neuroinflammatory tolerance in aged female rats compared to aged male rats, which is not explained by modulation of ovarian hormone signaling. Our results show a sex-specific shift in inflammatory milieu in the aged brain and meninges, which may protect aged females against prolonged behavioral deficits after inflammatory challenge. Future studies should explore sex differences in neuroimmune responses and behavior at later stages of aging and in preclinical models of neurodegenerative diseases to ascertain suitable intervention points and sex-specific immunotherapies to combat cognitive impairment.

Supplementary Material

Refer to Web version on PubMed Central for supplementary material.

Acknowledgements

This work was supported by the National Institute on Aging (R01AG062716, LKF; R01AG078758, LKF, LMI and ADG), National Institute of Neurological Disorders and Stroke (R01NS131806, ADG), and National Institute on Alcohol Abuse and Alcoholism (R01AA025591, KN; F32AA029928, JKM). Flow cytometry was performed at the Center for Biomedical Research Support Microscopy and Imaging Facility at UT Austin (RRID# SCR_021756). Library preparation, sequencing, and alignment for transcriptomic analyses were performed by the Genomic Sequencing and Analysis Facility at UT Austin.

Data availability

Data will be made available on request.

References

2022 Alzheimer's disease facts and figures. Alzheimers Dement. 2022;18(4):700–89. Epub 20220314. doi: 10.1002/alz.12638. [PubMed: 35289055]

Arevalo MA, Azcoitia I, Garcia-Segura LM. The neuroprotective actions of oestradiol and oestrogen receptors. Nat Rev Neurosci. 2015;16(1):17–29. Epub 2014/11/27. doi: 10.1038/nrn3856. [PubMed: 25423896]

Bachstetter AD, Van Eldik LJ, Schmitt FA, Neltner JH, Ighodaro ET, Webster SJ, Patel E, Abner EL, Kryscio RJ, Nelson PT. Disease-related microglia heterogeneity in the hippocampus of Alzheimer's disease, dementia with Lewy bodies, and hippocampal sclerosis of aging. Acta Neuropathol Commun. 2015;3(1):32. Epub 20150523. doi: 10.1186/s40478-015-0209-z. [PubMed: 26001591]

Barrientos RM, Frank MG, Hein AM, Higgins EA, Watkins LR, Rudy JW, Maier SF. Time course of hippocampal IL-1 beta and memory consolidation impairments in aging rats following peripheral infection. Brain Behav Immun. 2009;23(1):46–54. Epub 20080711. doi: 10.1016/j.bbi.2008.07.002. [PubMed: 18664380]

Barrientos RM, Hein AM, Frank MG, Watkins LR, Maier SF. Intracisternal interleukin-1 receptor antagonist prevents postoperative cognitive decline and neuroinflammatory response in aged rats. J Neurosci. 2012;32(42):14641–8. Epub 2012/10/19. doi: 10.1523/JNEUROSCI.2173-12.2012. [PubMed: 23077050]

Barrientos RM, Higgins EA, Biedenkapp JC, Sprunger DB, Wright-Hardesty KJ, Watkins LR, Rudy JW, Maier SF, 2006. Peripheral infection and aging interact to impair hippocampal memory consolidation. Neurobiology of Aging 27 (5), 723–732. 10.1016/j.neurobiolaging.2005.03.010. [PubMed: 15893410]

Benedusi V, Meda C, Della Torre S, Monteleone G, Vegeto E, Maggi A. A lack of ovarian function increases neuroinflammation in aged mice. Endocrinology. 2012;153(6): 2777–88. Epub 20120404. doi: 10.1210/en.2011-1925. [PubMed: 22492304]

Bisht K, Sharma KP, Lecours C, Sánchez MG, El Hajj H, Milior G, Olmos-Alonso A, Gómez-Nicola D, Luheshi G, Vallières L, Branchi I, Maggi L, Limatola C, Butovsky O, Tremblay M. Dark microglia: A new phenotype predominantly associated with pathological states. Glia. 2016;64(5):826–39. Epub 20160205. doi: 10.1002/glia.22966. [PubMed: 26847266]

Bonham LW, Sirkis DW, Yokoyama JS. The Transcriptional Landscape of Microglial Genes in Aging and Neurodegenerative Disease. Front Immunol. 2019;10:1170. Epub 20190604. doi: 10.3389/fimmu.2019.01170. [PubMed: 31214167]

Broux B, Pannemans K, Zhang X, Markovic-Plese S, Broekmans T, Eijnde BO, Van Wijmeersch B, Somers V, Geusens P, van der Pol S, van Horssen J, Stinissen P, Hellings N. CX(3)CR1 drives cytotoxic CD4(+)CD28(−) T cells into the brain of multiple sclerosis patients. J Autoimmun. 2012;38(1):10–9. Epub 20111126. doi: 10.1016/j.jaut.2011.11.006. [PubMed: 22123179]

Corbo RM, Gambina G, Broggio E, Scacchi R. Influence of variation in the follicle-stimulating hormone receptor gene (FSHR) and age at menopause on the development of Alzheimer's disease in women. Dement Geriatr Cogn Disord. 2011; 32(1):63–9. Epub 20110824. doi: 10.1159/000330472. [PubMed: 21865747]

Corona AW, Huang Y, O'Connor JC, Dantzer R, Kelley KW, Popovich PG, Godbout JP, 2010. Fractalkine receptor (CX3CR1) deficiency sensitizes mice to the behavioral changes induced by lipopolysaccharide. Journal of Neuroinflammation 7, 93. 10.1186/1742-2094-7-93. [PubMed: 21167054]

Coughlan GT, Betthauser TJ, Boyle R, Koscik RL, Klinger HM, Chibnik LB, Jonaitis EM, Yau WW, Wenzel A, Christian BT, Gleason CE, Saelzler UG, Properzi MJ, Schultz AP, Hanseeuw BJ, Manson JE, Rentz DM, Johnson KA, Sperling R, Johnson SC, Buckley RF, 2023. Association of age at menopause and hormone therapy Use with tau and beta-Amyloid positron emission

tomography. JAMA Neurology 80 (5), 462–473. 10.1001/jamaneurol.2023.0455. [PubMed: 37010830]

Davies DS, Ma J, Jegathees T, Goldsbury C. Microglia show altered morphology and reduced arborization in human brain during aging and Alzheimer's disease. Brain Pathol. 2017;27(6):795–808. Epub 20161212. doi: 10.1111/bpa.12456. [PubMed: 27862631]

Davis BM, Salinas-Navarro M, Cordeiro MF, Moons L, De Groef L. Characterizing microglia activation: a spatial statistics approach to maximize information extraction. Sci Rep. 2017;7(1):1576. Epub 20170508. doi: 10.1038/s41598-017-01747-8. [PubMed: 28484229]

Doran SJ, Ritzel RM, Glaser EP, Henry RJ, Faden AI, Loane DJ. Sex Differences in Acute Neuroinflammation after Experimental Traumatic Brain Injury Are Mediated by Infiltrating Myeloid Cells. J Neurotrauma. 2019;36(7):1040–53. Epub 20181116. doi: 10.1089/neu.2018.6019. [PubMed: 30259790]

Dorfman MD, Krull JE, Douglass JD, Fasnacht R, Lara-Lince F, Meek TH, Shi X, Damian V, Nguyen HT, Matsen ME, Morton GJ, Thaler JP. Sex differences in microglial CX3CR1 signalling determine obesity susceptibility in mice. Nat Commun. 2017;8 (1):14556. Epub 20170222. doi: 10.1038/ncomms14556. [PubMed: 28223698]

Dulken BW, Buckley MT, Navarro Negredo P, Saligrama N, Cayrol R, Leeman DS, George BM, Boutet SC, Hebestreit K, Pluvinage JV, Wyss-Coray T, Weissman IL, Vogel H, Davis MM, Brunet A, 2019. Single-cell analysis reveals T cell infiltration in old neurogenic niches. Nature 571 (7764), 205–210. 10.1038/s41586-019-1362-5. [PubMed: 31270459]

Fischinger S, Boudreau CM, Butler AL, Streeck H, Alter G. Sex differences in vaccine-induced humoral immunity. Semin Immunopathol. 2019;41(2):239–49. Epub 20181213. doi: 10.1007/s00281-018-0726-5. [PubMed: 30547182]

Fonken LK, Kitt MM, Gaudet AD, Barrientos RM, Watkins LR, Maier SF. Diminished circadian rhythms in hippocampal microglia may contribute to age-related neuroinflammatory sensitization. Neurobiol Aging. 2016;47:102–12. Epub 20160801. doi: 10.1016/j.neurobiolaging.2016.07.019. [PubMed: 27568094]

Fonken LK, Frank MG, D'Angelo HM, Heinze JD, Watkins LR, Lowry CA, Maier SF. Mycobacterium vaccae immunization protects aged rats from surgery-elicited neuroinflammation and cognitive dysfunction. Neurobiol Aging. 2018;71:105–14. Epub 20180724. doi: 10.1016/j.neurobiolaging.2018.07.012. [PubMed: 30118926]

Fonken LK, Frank MG, Gaudet AD, D'Angelo HM, Daut RA, Hampson EC, Ayala MT, Watkins LR, Maier SF. Neuroinflammatory priming to stress is differentially regulated in male and female rats. Brain Behav Immun. 2018;70:257–67. Epub 20180307. doi: 10.1016/j.bbi.2018.03.005. [PubMed: 29524458]

Fonken LK, Frank MG, Kitt MM, D'Angelo HM, Norden DM, Weber MD, Barrientos RM, Godbout JP, Watkins LR, Maier SF, 2016b. The alarmin HMGB1 mediates Age-Induced neuroinflammatory priming. The Journal of Neuroscience 36 (30), 7946–7956. 10.1523/JNEUROSCI.1161-16.2016. [PubMed: 27466339]

Frank MG, Wieseler-Frank JL, Watkins LR, Maier SF. Rapid isolation of highly enriched and quiescent microglia from adult rat hippocampus: immunophenotypic and functional characteristics. J Neurosci Methods. 2006;151(2):121–30. Epub 20050824. doi: 10.1016/j.jneumeth.2005.06.026. [PubMed: 16125247]

Frank MG, Barrientos RM, Watkins LR, Maier SF. Aging sensitizes rapidly isolated hippocampal microglia to LPS ex vivo. J Neuroimmunol. 2010;226(1–2):181–4. Epub 20100526. doi: 10.1016/j.jneuroim.2010.05.022. [PubMed: 20537730]

Gleicher N, Barad DH. Gender as risk factor for autoimmune diseases. J Autoimmun. 2007;28(1):1–6. Epub 20070129. doi: 10.1016/j.jaut.2006.12.004. [PubMed: 17261360]

Gubbels Bupp MR, Potluri T, Fink AL, Klein SL. The Confluence of Sex Hormones and Aging on Immunity. Front Immunol. 2018;9(1664–3224 (Print)):1269. Epub 20180604. doi: 10.3389/fimmu.2018.01269. [PubMed: 29915601]

Guillot-Sestier MV, Araiz AR, Mela V, Gaban AS, O'Neill E, Joshi L, Chouchani ET, Mills EL, Lynch MA. Microglial metabolism is a pivotal factor in sexual dimorphism in Alzheimer's disease. Commun Biol. 2021;4(1):711. Epub 20210610. doi: 10.1038/s42003-021-02259-y. [PubMed: 34112929]

Hammond TR, Dufort C, Dissing-Olesen L, Giera S, Young A, Wysoker A, Walker AJ, Gergits F, Segel M, Nemesh J, Marsh SE, Saunders A, Macosko E, Ginhoux F, Chen J, Franklin RJM, Piao X, McCarroll SA, Stevens B. Single-Cell RNA Sequencing of Microglia throughout the Mouse Lifespan and in the Injured Brain Reveals Complex Cell-State Changes. Immunity. 2019;50(1):253–71 e6. Epub 20181121. doi: 10.1016/j.immuni.2018.11.004. [PubMed: 30471926]

Hirokawa K, Utsuyama M, Hayashi Y, Kitagawa M, Makinodan T, Fulop T. Slower immune system aging in women versus men in the Japanese population. Immun Ageing. 2013;10(1):19. Epub 20130515. doi: 10.1186/1742-4933-10-19. [PubMed: 23675689]

Hou Y, Dan X, Babbar M, Wei Y, Hasselbalch SG, Croteau DL, Bohr VA, 2019. Ageing as a risk factor for neurodegenerative disease. Nature Reviews Neurology. 15 (10), 565–581. 10.1038/s41582-019-0244-7. [PubMed: 31501588]

Kaya T, Mattugini N, Liu L, Ji H, Cantuti-Castelvetri L, Wu J, Schifferer M, Groh J, Martini R, Besson-Girard S, Kaji S, Liesz A, Gokce O, Simons M. CD8(+) T cells induce interferon-responsive oligodendrocytes and microglia in white matter aging. Nat Neurosci. 2022;25(11):1446–57. Epub 20221024. doi: 10.1038/s41593-022-01183-6. [PubMed: 36280798]

Kipnis J, Cohen H, Cardon M, Ziv Y, Schwartz M. T cell deficiency leads to cognitive dysfunction: implications for therapeutic vaccination for schizophrenia and other psychiatric conditions. Proc Natl Acad Sci U S A. 2004;101(21):8180–5. Epub 20040512. doi: 10.1073/pnas.0402268101. [PubMed: 15141078]

Kireev RA, Vara E, Vina J, Tresguerres JA. Melatonin and oestrogen treatments were able to improve neuroinflammation and apoptotic processes in dentate gyrus of old ovariectomized female rats. Age (Dordr). 2014;36(5):9707. Epub 20140819. doi: 10.1007/s11357-014-9707-3. [PubMed: 25135305]

Klein SL, Flanagan KL. Sex differences in immune responses. Nat Rev Immunol. 2016;16 (10):626–38. Epub 20160822. doi: 10.1038/nri.2016.90. [PubMed: 27546235]

Koebele SV, Bimonte-Nelson HA. Modeling menopause: The utility of rodents in translational behavioral endocrinology research. Maturitas. 2016;87:5–17. Epub 20160203. doi: 10.1016/j.maturitas.2016.01.015. [PubMed: 27013283]

Levine DA, Gross AL, Briceno EM, Tilton N, Giordani BJ, Sussman JB, Hayward RA, Burke JF, Hingtgen S, Elkind MSV, Manly JJ, Gottesman RF, Gaskin DJ, Sidney S, Sacco RL, Tom SE, Wright CB, Yaffe K, Galecki AT. Sex Differences in Cognitive Decline Among US Adults. JAMA Netw Open. 2021;4(2):e210169. Epub 20210201. doi: 10.1001/jamanetworkopen.2021.0169. [PubMed: 33630089]

Li YJ, Scott WK, Hedges DJ, Zhang F, Gaskell PC, Nance MA, Watts RL, Hubble JP, Koller WC, Pahwa R, Stern MB, Hiner BC, Jankovic J, Allen FA Jr., Goetz CG, Mastaglia F, Stajich JM, Gibson RA, Middleton LT, Saunders AM, Scott BL, Small GW, Nicodemus KK, Reed AD, Schmechel DE, Welsh-Bohmer KA, Conneally PM, Roses AD, Gilbert JR, Vance JM, Haines JL, Pericak-Vance MA. Age at onset in two common neurodegenerative diseases is genetically controlled. Am J Hum Genet. 2002;70(4): 985–93. Epub 20020301. doi: 10.1086/339815. [PubMed: 11875758]

Lier J, Streit WJ, Bechmann I, 2021. Beyond activation: Characterizing microglial functional phenotypes. Cells [Internet]. 10 9.

Limatola C, Ransohoff RM. Modulating neurotoxicity through CX3CL1/CX3CR1 signaling. Front Cell Neurosci. 2014;8:229. Epub 20140808. doi: 10.3389/fncel.2014.00229. [PubMed: 25152714]

Liston A, Dooley J, Yshii L. Brain-resident regulatory T cells and their role in health and disease. Immunol Lett. 2022;248:26–30. Epub 20220610. doi: 10.1016/j.imlet.2022.06.005. [PubMed: 35697195]

Liston A, Yshii L, 2023. T cells drive aging of the brain. Nature Immunology 24 (1), 12–13. 10.1038/s41590-022-01390-0. [PubMed: 36596892]

Livak KJ, Schmittgen TD, 2001. Analysis of relative gene expression data using real-time quantitative PCR and the 2(-Delta delta c(T)) method. Methods 25 (4), 402–408. 10.1006/meth.2001.1262. [PubMed: 11846609]

Lord JM. The effect of ageing of the immune system on vaccination responses. Hum Vaccin Immunother. 2013;9(6):1364–7. Epub 20130412. doi: 10.4161/hv.24696. [PubMed: 23584248]

Manglani M, Gossa S, McGavern DB, 2018. Leukocyte isolation from brain, spinal cord, and meninges for flow cytometric analysis. Current Protocols in Immunology 121 (1), e44. [PubMed: 30040211]

Marschallinger J, Iram T, Zardeneta M, Lee SE, Lehallier B, Haney MS, Pluvinage JV, Mathur V, Hahn O, Morgens DW, Kim J, Tevini J, Felder TK, Wolinski H, Bertozzi CR, Bassik MC, Aigner L, Wyss-Coray T. Lipid-droplet-accumulating microglia represent a dysfunctional and proinflammatory state in the aging brain. Nat Neurosci. 2020;23(2):194–208. Epub 20200120. doi: 10.1038/s41593-019-0566-1. [PubMed: 31959936]

Muscat SM, Butler MJ, Mackey-Alfonso SE, Barrientos RM. Young adult and aged female rats are vulnerable to amygdala-dependent, but not hippocampus-dependent, memory impairment following short-term high-fat diet. Brain Res Bull. 2023;195: 145–56. Epub 20230302. doi: 10.1016/j.brainresbull.2023.03.001. [PubMed: 36870621]

Pardo J, Abba MC, Lacunza E, Francelle L, Morel GR, Outeiro TF, Goya RG. Identification of a conserved gene signature associated with an exacerbated inflammatory environment in the hippocampus of aging rats. Hippocampus. 2017;27(4):435–49. Epub 20170123. doi: 10.1002/hipo.22703. [PubMed: 28085212]

Preissler J, Grosche A, Lede V, Le Duc D, Krugel K, Matyash V, Szulzewsky F, Kallendrusch S, Immig K, Kettenmann H, Bechmann I, Schoneberg T, Schulz A. Altered microglial phagocytosis in GPR34-deficient mice. Glia. 2015;63(2):206–15. Epub 20140820. doi: 10.1002/glia.22744. [PubMed: 25142016]

Rayasam A, Kijak JA, Dallmann M, Hsu M, Zindl N, Lindstedt A, Steinmetz L, Harding JS, Harris MG, Karman J, Sandor M, Fabry Z. Regional Distribution of CNS Antigens Differentially Determines T-Cell Mediated Neuroinflammation in a CX3CR1-Dependent Manner. J Neurosci. 2018;38(32):7058–71. Epub 20180629. doi: 10.1523/JNEUROSCI.0366-18.2018. [PubMed: 29959236]

Reagin KL, Funk KE. The role of antiviral CD8(+) T cells in cognitive impairment. Curr Opin Neurobiol. 2022;76(1873–6882 (Electronic)):102603. Epub 20220708. doi: 10.1016/j.conb.2022.102603. [PubMed: 35810534]

Sanchez K, Wu SL, Kakkar R, Darling JS, Harper CS, Fonken LK. Ovariectomy in mice primes hippocampal microglia to exacerbate behavioral sickness responses. Brain Behav Immun Health. 2023;30:100638. Epub 20230518. doi: 10.1016/j.bbih.2023.100638. [PubMed: 37256192]

Sasaki S, Sullivan M, Narvaez CF, Holmes TH, Furman D, Zheng NY, Nishtala M, Wrammert J, Smith K, James JA, Dekker CL, Davis MM, Wilson PC, Greenberg HB, He XS. Limited efficacy of inactivated influenza vaccine in elderly individuals is associated with decreased production of vaccine-specific antibodies. J Clin Invest. 2011;121(8):3109–19. Epub 20110725. doi: 10.1172/JCI57834. [PubMed: 21785218]

Sayo A, Konishi H, Kobayashi M, Kano K, Kobayashi H, Hibi H, Aoki J, Kiyama H. GPR34 in spinal microglia exacerbates neuropathic pain in mice. J Neuroinflammation. 2019;16(1):82. Epub 20190411. doi: 10.1186/s12974-019-1458-8. [PubMed: 30975169]

Scheiblich H, Trombly M, Ramirez A, Heneka MT. Neuroimmune Connections in Aging and Neurodegenerative Diseases. Trends Immunol. 2020;41(4):300–12. Epub 20200305. doi: 10.1016/j.it.2020.02.002. [PubMed: 32147113]

Spencer SJ, D'Angelo H, Soch A, Watkins LR, Maier SF, Barrientos RM. High-fat diet and aging interact to produce neuroinflammation and impair hippocampal- and amygdalar-dependent memory. Neurobiol Aging. 2017;58:88–101. Epub 20170624. doi: 10.1016/j.neurobiolaging.2017.06.014. [PubMed: 28719855]

Stratoulias V, Venero JL, Tremblay ME, Joseph B. Microglial subtypes: diversity within the microglial community. EMBO J. 2019;38(17):e101997. Epub 20190802. doi: 10.15252/embj.2019101997. [PubMed: 31373067]

Wiedrick J, Meza-Romero R, Gerstner G, Seifert H, Chaudhary P, Headrick A, Kent G, Maestas A, Offner H, Vandenbark AA. Sex differences in EAE reveal common and distinct cellular and molecular components. Cell Immunol. 2021;359(1090–2163 (Electronic)):104242. Epub 20201022. doi: 10.1016/j.cellimm.2020.104242. [PubMed: 33190849]

Wood SH, Craig T, Li Y, Merry B, de Magalhaes JP. Whole transcriptome sequencing of the aging rat brain reveals dynamic RNA changes in the dark matter of the genome. Age (Dordr). 2013;35(3):763–76. Epub 20120504. doi: 10.1007/s11357-012-9410-1. [PubMed: 22555619]

Xu YZ, Nygard M, Kristensson K, Bentivoglio M. Regulation of cytokine signaling and T-cell recruitment in the aging mouse brain in response to central inflammatory challenge. Brain Behav Immun. 2010;24(1):138–52. Epub 20090916. doi: 10.1016/j.bbi.2009.09.006. [PubMed: 19765643]

Zhang X, Wang R, Chen H, Jin C, Jin Z, Lu J, Xu L, Lu Y, Zhang J, Shi L. Aged microglia promote peripheral T cell infiltration by reprogramming the microenvironment of neurogenic niches. Immun Ageing. 2022;19(1):34. Epub 20220725. doi: 10.1186/s12979-022-00289-6. [PubMed: 35879802]

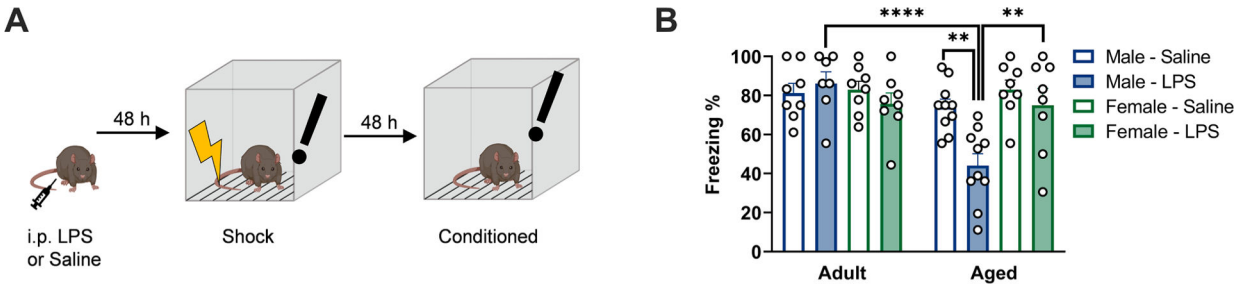

Fig. 1.

Aged male, but not aged female, rats exhibit impaired contextual fear memory following LPS administration. a) Experimental protocol: Rats were administered 40 μg lipopolysaccharide (LPS) or saline vehicle via intraperitoneal injection, followed by memory assessment via fear conditioning protocol. Fear conditioning was performed by shock exposure 48 h after LPS injection, followed by assessment of freezing behavior in the conditioned context 48 h later (96 h post-LPS). Schematic created with Biorender.com. b) Aged male rats exhibited a significant reduction in freezing behavior upon re-exposure to the conditioned context. n = 8–10. ** $p < 0.01$, **** $p < 0.0001$.

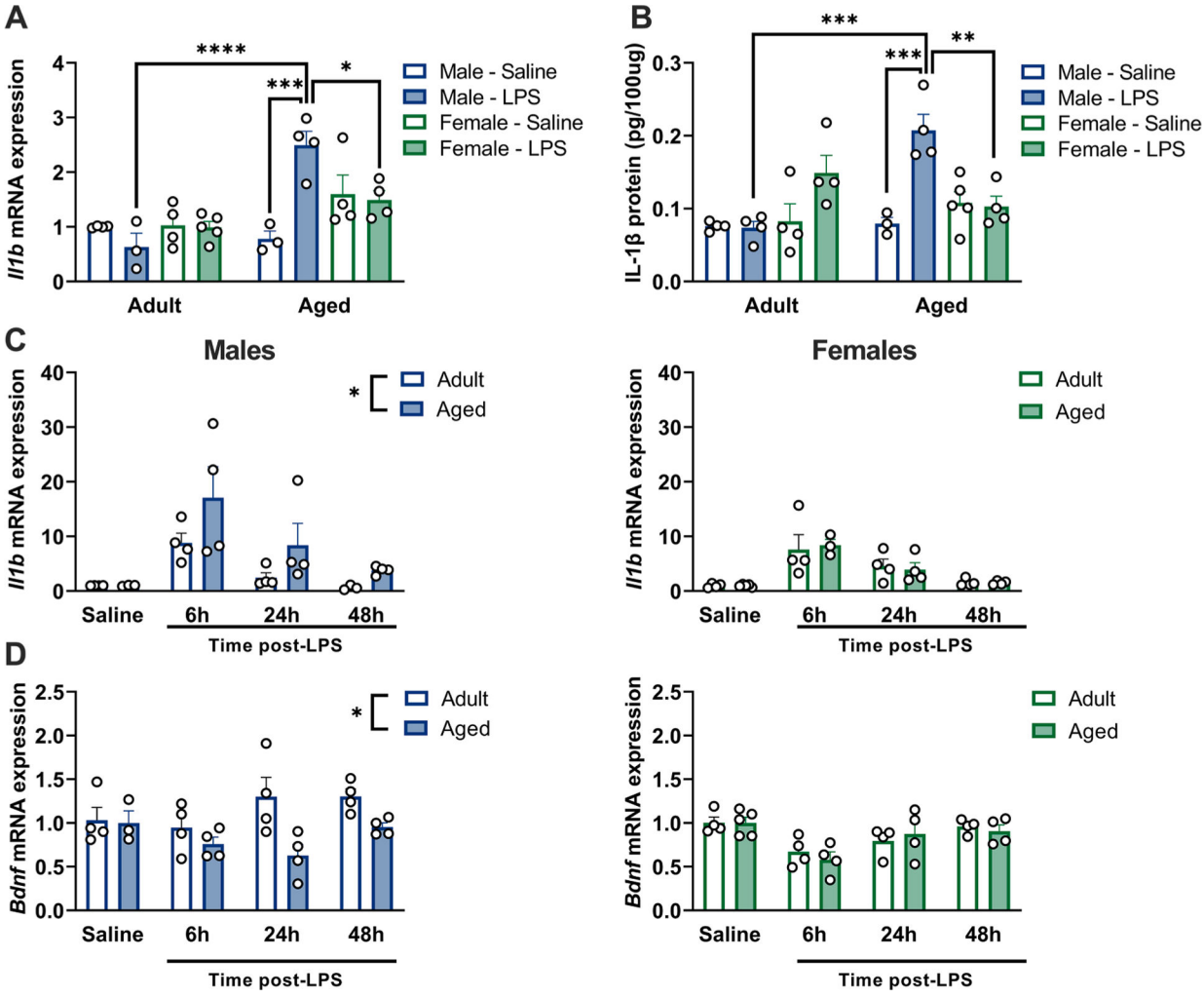

Fig. 2.

Aged male, but not female, rats exhibit increases in IL-1β 48 h following LPS. a) Expression of *Il1b* mRNA is significantly elevated in aged male, but not female, hippocampi 48 h following LPS. Results normalized to the adult male saline group, n = 3–5. b) IL-1β protein concentration is significantly elevated in aged male, but not female, hippocampi 48 h following LPS. n = 3–5. c) *Il1b* mRNA expression is persistently elevated in aged male hippocampi (left) following LPS challenge but not in aged females (right). Males and females are plot separately to aid visualization, all results normalized to adult male saline control group, n = 3–5. d) *Bdnf* mRNA expression is reduced in aged male hippocampi following LPS challenge (left) but not in aged females (right). Males and females are plot separately to aid visualization, all results normalized to adult male saline control group, n = 3–5. * $p < 0.05$, ** $p < 0.01$, *** $p < 0.001$, **** $p < 0.0001$.

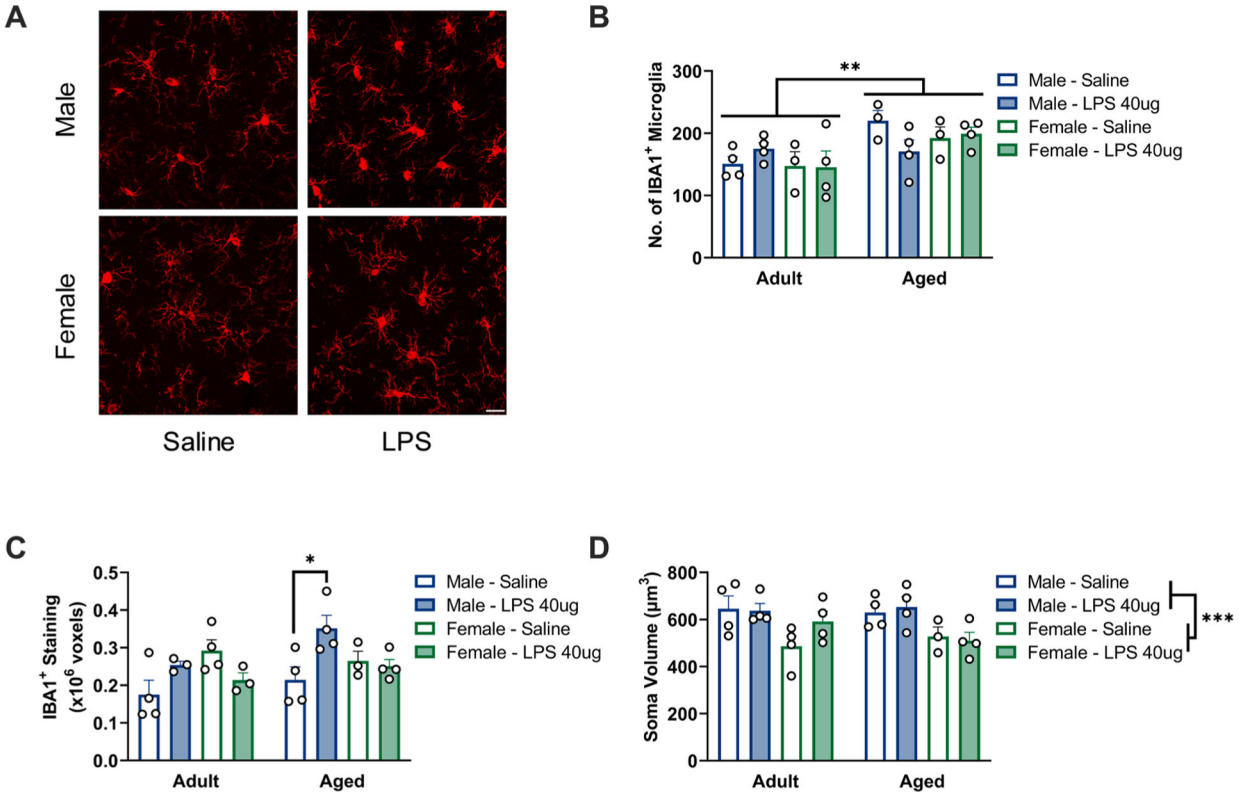

Fig. 3.

Microglia in aged male, but not aged female, hippocampi show morphological features of inflammatory priming. a) Representative images from the dentate gyrus of aged animals. Scale bar = 20 µm. b) An increased number of IBA1$^+$ microglia was observed in the dentate gyrus of aged animals, ROI: 0.63×0.63 mm, n = 3–4. c) Aged males showed an increase in the area of IBA1$^+$ staining within the dentate gyrus, n = 3–4. d) Males exhibited a larger average soma volume than females in the dentate gyrus, n = 3–4. * $p < 0.05$, ** $p < 0.01$, *** $p < 0.001$.

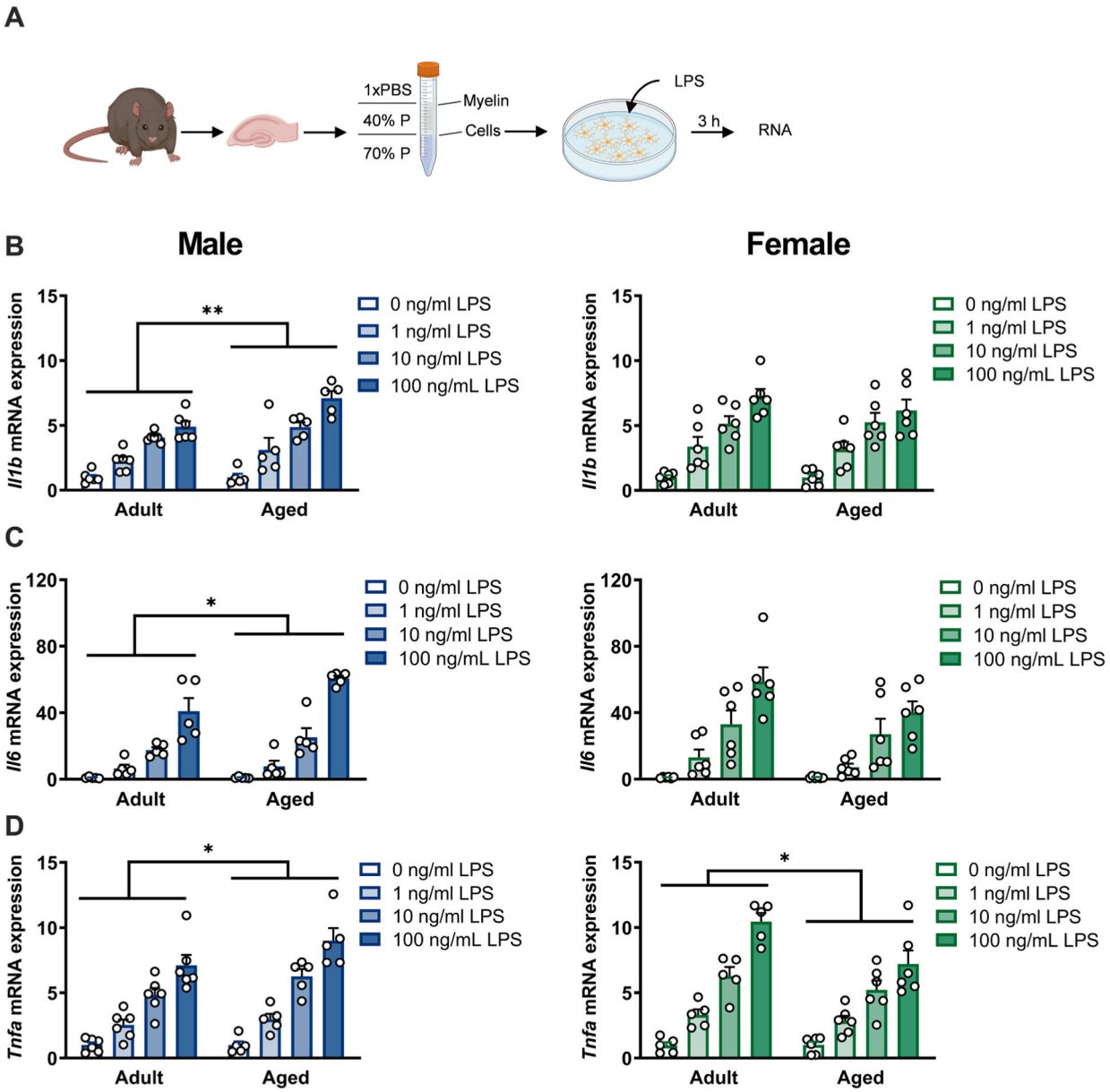

Fig. 4.

Microglia isolated from aged male, but not female, rats exhibit potentiated inflammatory responses indicative of a "primed" state. a) Experimental protocol: Hippocampi were isolated from rats and microglia purified via density centrifugation in discontinuous Percoll (P) gradient. Microglia were stimulated with varying doses of LPS ex vivo for 3 h, followed by RNA extraction. Schematic created with Biorender.com. b) Microglia from aged males (left), but not aged females (right) exhibited an enhanced production of *Il1b* mRNA in response to LPS stimulation. Results normalized within each sex to adult 0 ng/ml control group, n = 5–6. c) Microglia from aged males (left), but not aged females (right) exhibited an enhanced production of *Il6* mRNA in response to LPS stimulation. Results normalized within each sex to adult 0 ng/ml group, n = 5–6. d) Microglia from aged males (left) exhibited an enhanced production of *Tnfa* mRNA in response to LPS stimulation, whereas

microglia from aged females (right) show a decreased production of *Tnfa* mRNA. Results normalized within each sex to adult 0 ng/ml group, n = 5–6. * $p < 0.05$, ** $p < 0.01$.

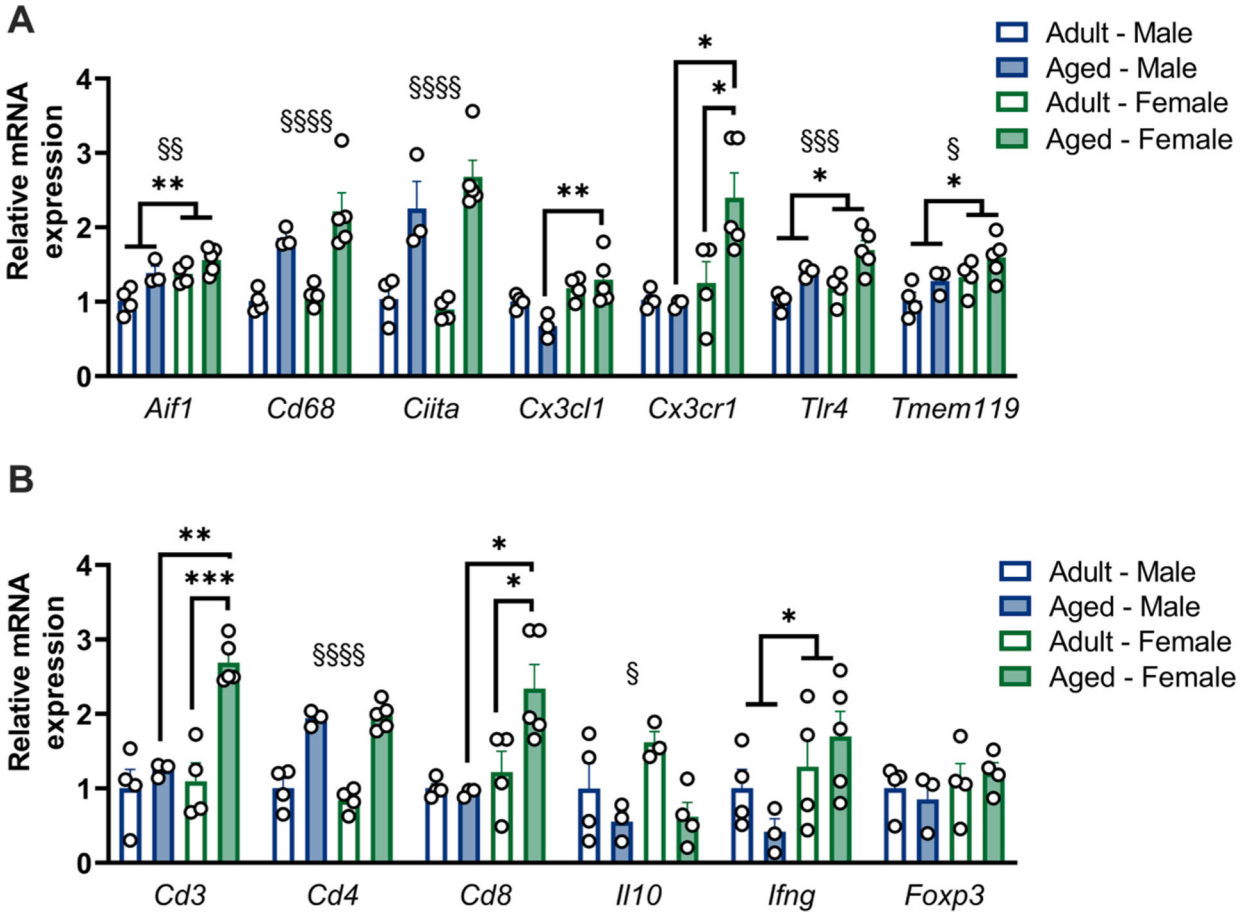

Fig. 5.

Neuroinflammatory pathway genes are regulated by both age and sex. a) qPCR analysis of microglia-related genes in the hippocampus at baseline. A subset of genes (*Cd68*, *Ciita*) are increased with aging in both sexes, whereas *Tlr4* and *Cx3cr1* are increased with aging in females alone. *Aif1* is increased in adult females relative to adult males, and both *Cx3cl1* and *Cx3cr1* are increased in aged females relative to aged males. Results normalized to adult male group for each gene, n = 3–4. b) qPCR analysis of T cell-related genes in the hippocampus at baseline. Both *Cd3* and *Cd8* show specific upregulation in aged females compared to both adult females and aged males, *Cd4* expression was increased with age in both sexes. Results normalized to adult male group for each gene, n = 3–4. * $p < 0.05$, ** $p < 0.01$, *** $p < 0.001$, **** $p < 0.0001$. § denotes main effect of age.

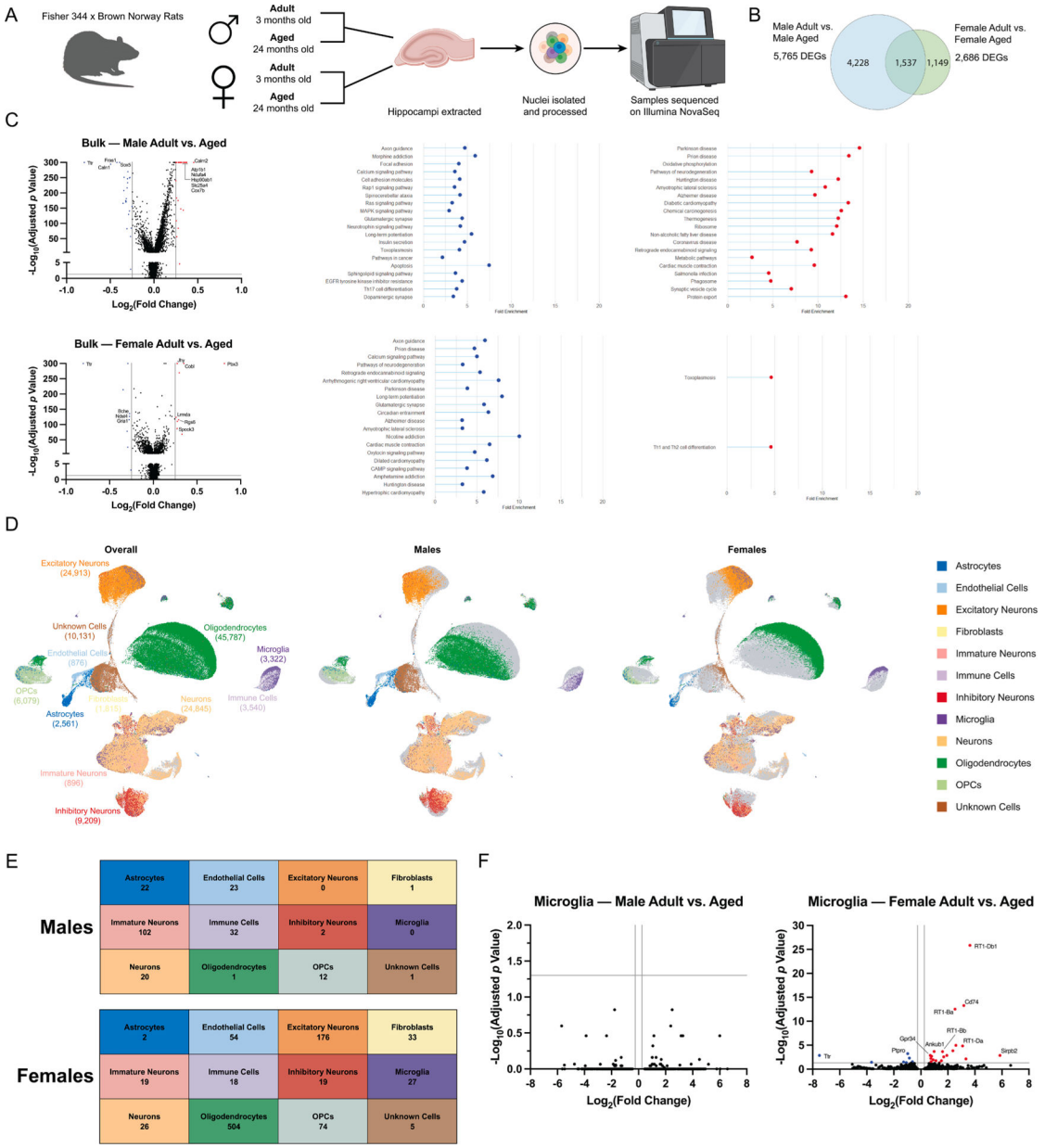

Fig. 6.

Sexual dimorphism in age-dependent changes in the hippocampal transcriptome. a) Experimental protocol. Schematic created with Biorender.com. b) Venn diagram of differentially expressed genes identified from bulk sequencing of hippocampi from adult and aged male (left) and female (right) rats. c) Volcano plots and KEGG analysis of bulk sequencing of hippocampi from adult and aged male (top) and female (bottom) rats. The top 20 significantly enriched pathways are displayed for each sex: red – upregulated pathways, blue – downregulated pathways. d) UMAP analysis of single cell sequencing to identify cell populations (left) and compare adult vs aged males (center) and adult vs aged females (right). e) Summary of differentially-expressed genes in cell populations from males (top)

and females (bottom). f) Volcano plots of differentially-expressed genes in microglia from adult and aged male (left) and female (right) rats.

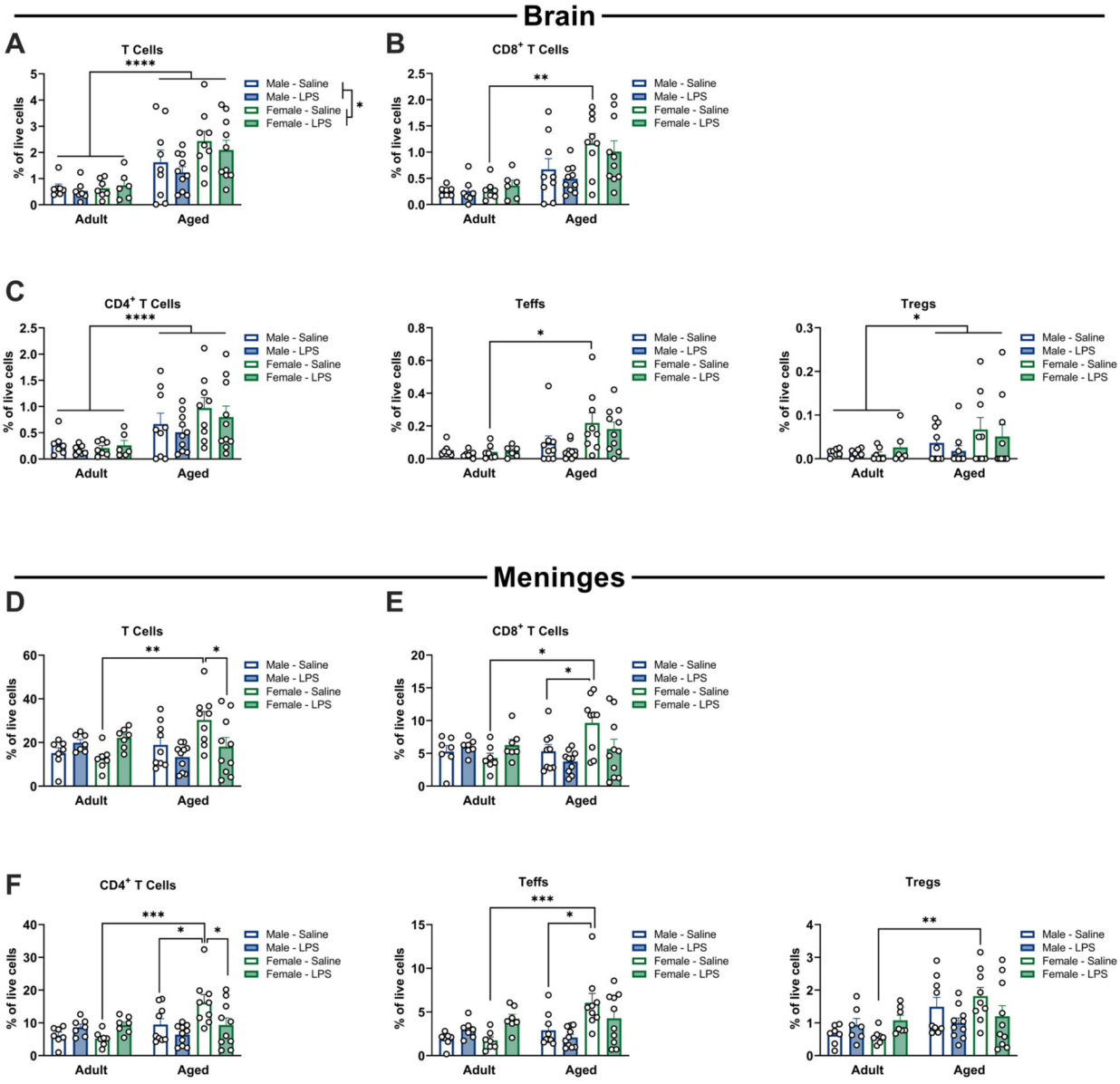

Fig. 7.

Sex-, age- and inflammation-dependent increases in T cell populations in the brain and meninges. Flow cytometry of brain tissue 48 h following i.p. LPS or saline, analyzed for T cell subpopulations. A significant increase in cell numbers (as a % of live cells) was observed in aged females compared to adult females at baseline for total T cells (a), CD8+ cytotoxic T cells (b), CD4+ T helper cells (total CD4+ – c, left) and CD4 + effector cells (CD4+ CD25+ FoxP3− – c, center), but not in Tregs (CD4+ CD25+ FoxP3+ – c, right), n = 6–10. Flow cytometry of meninges 48 h following i.p. LPS or saline, analyzed for T cell subpopulations. A significant increase in cell numbers (as a % of live cells) was observed in aged females compared to adult females at baseline for total T cells (d), CD8+ cytotoxic T cells (e), CD4+ T helper cells (total CD4+ – f, left) and CD4+ effector cells (CD4+ CD25+ FoxP3 – f, center), and in Tregs (CD4+ CD25+ FoxP3+ – f, right). Aged females also showed an increase in CD8+, CD4+ and effector CD4+ cells relative to aged males at

baseline, and an increase in total T cells and CD4+ cells relative to aged females given LPS, n = 7–10. * $p < 0.05$, ** $p < 0.01$, *** $p < 0.001$.

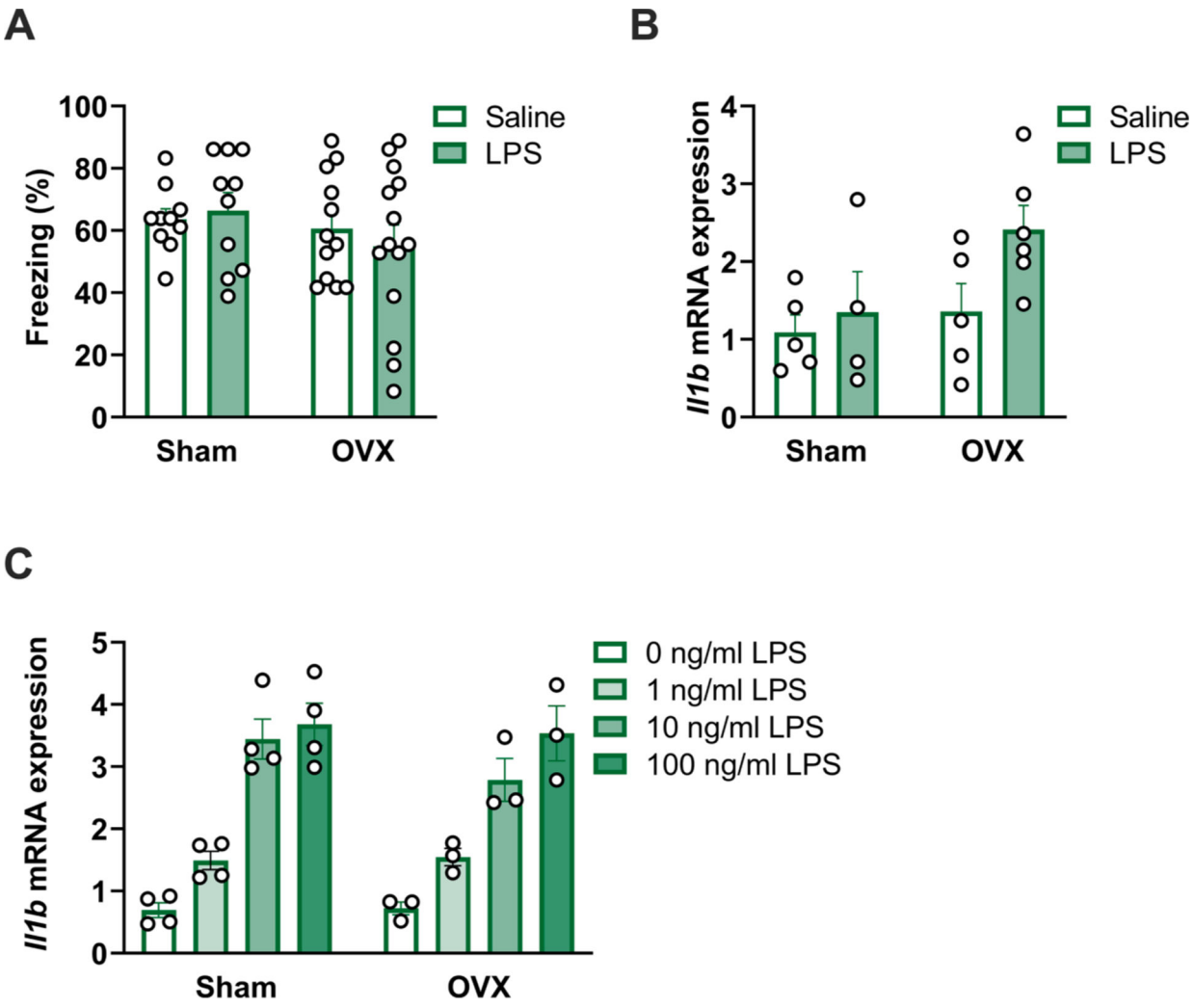

Fig. 8.

Ovariectomy does not potentiate age-associated neuroinflammation in female rats. a) Ovariectomized (OVX) and sham-operated aged female rats were assessed for memory function via fear conditioning following 40 μg LPS or saline (control) i.p. injection (assessment 48 h following shock exposure and 96 h following injections). OVX did not potentiate a memory deficit following LPS or saline (control) administration ($p > 0.05$), n = 9–14. b) OVX did not exacerbate hippocampal *Il1b* expression in aged females following LPS administration or at baseline ($p > 0.05$), n = 4–5. c) OVX did not potentiate inflammatory responses in isolated microglia from aged female rats ($p > 0.05$), n = 3–4.